MEMORANDUM REPORT BRL-MR-3823

BRL

A COMPARISON OF DAMAGE FUNCTIONS FOR USE IN ARTILLERY EFFECTIVENESS CODES

J. TERRENCE KLOPCIC

APRIL 1990

U.S. ARMY LABORATORY COMMAND

BALLISTIC RESEARCH LABORATORY
ABERDEEN PROVING GROUND, MARYLAND

Destroy this report when it is no longer needed. DO NOT return it to the originator.

Additional copies of this report may be obtained from the National Technical Information Service, U.S. Department of Commerce, 5285 Port Royal Road, Springfield, VA 22161.

The findings of this report are not to be construed as an official Department of the Army position, unless so designated by other authorized documents.

The use of trade names or manufacturers' names in this report does not constitute indorsement of any commercial product.

UNCLASSIFIED

REPORT DOCUMENTATION PAGE

Form Approved
OMB No. 0704-0188

1. AGENCY USE ONLY (Leave blank)	2. REPORT DATE	3. REPORT TYPE AND DATES COVERED
	April 1990	Final, Sept 89-Jan 90

4. TITLE AND SUBTITLE
A Comparison of Damage Functions for Use in Artillery Effectiveness Codes

5. FUNDING NUMBERS
1L162618AH80
DA31 6061

6. AUTHOR(S)
J. TERRENCE KLOPCIC

7. PERFORMING ORGANIZATION NAME(S) AND ADDRESS(ES)

8. PERFORMING ORGANIZATION REPORT NUMBER

9. SPONSORING/MONITORING AGENCY NAME(S) AND ADDRESS(ES)
Ballistic Research Laboratory
ATTN: SLCBR-DD-T
Aberdeen Proving Ground, MD 21005-5066

10. SPONSORING/MONITORING AGENCY REPORT NUMBER
BRL-MR-3823

11. SUPPLEMENTARY NOTES

12a. DISTRIBUTION/AVAILABILITY STATEMENT
Distribution is Unlimited.

12b. DISTRIBUTION CODE

13. ABSTRACT (Maximum 200 words)

This report has three sections. The first section presents a comparison of results from the Carleton and Cookie Cutter functions, including both a mathematical proof and numerical demonstration of their relationships. The second section defines and develops the hybrid (Klopcic) function. Finally, the third section presents some numerical examples of simulations which demonstrate failures of the Carleton/CC functions and compares the behavior of the Klopcic function.

14. SUBJECT TERMS
Vulnerability Tank
Fault-Free
Methodology

15. NUMBER OF PAGES
66

16. PRICE CODE

17. SECURITY CLASSIFICATION OF REPORT	18. SECURITY CLASSIFICATION OF THIS PAGE	19. SECURITY CLASSIFICATION OF ABSTRACT	20. LIMITATION OF ABSTRACT
UNCLASSIFIED	UNCLASSIFIED	UNCLASSIFIED	SAR

INTENTIONALLY LEFT BLANK.

Contents

This page intentionally left blank

List of Figures

List of Tables

This page intentionally left blank

I. Introduction

A. Background

In mathematical combat simulation, it is common to model indirect fire (area) weapons in two independent steps: First, specific detonation points of the incoming warheads are selected using Monte Carlo methods. Then, each target element is located with respect to each warhead detonation point and the probability of achieving some level(s) of damage are determined, usually from the separation and orientation of each warhead-target pair. In practical cases, closed form functions are used to calculate the probability of damage. These functions are most often in one of two forms: the Carleton-von Neumann (Carleton) and the Cookie-Cutter (CC) forms. These two functional forms are shown in Figure 1.

Indirect fire simulations of this type are commonly done in the BRL, especially as an intrinsic part of analyses using the AURA methodology.[1] When attention was turned toward new, more accurate weaponry, it was seen that the apparent effectiveness of two otherwise identical weapons might be significantly different if a Carleton were used for one and a CC for the other. This observation led to the present study of the Carleton and Cookie Cutter, the formulation of a hybrid function (the "Klopcic" function) and the development of a user-friendly, menu-driven computer code to calculate the effectiveness of artillery attacks upon collections of different targets.

B. Scope

This report has three sections. The first section presents a comparison of results from the Carleton and Cookie Cutter functions, including both a mathematical proof and a numerical demonstration of their relationships. The second section defines and develops the hybrid (Klopcic) function. Finally, the third section presents some numerical examples of simulations which demonstrate failures of the Carleton/CC functions and compares the behavior of the Klopcic function.

[1] J. Terrence Klopcic, *Input Manual for the Army Unit Resiliency Analysis (AURA) Methodology: 1988 Update*, BRL Report BRL-TR-2914, May 1988

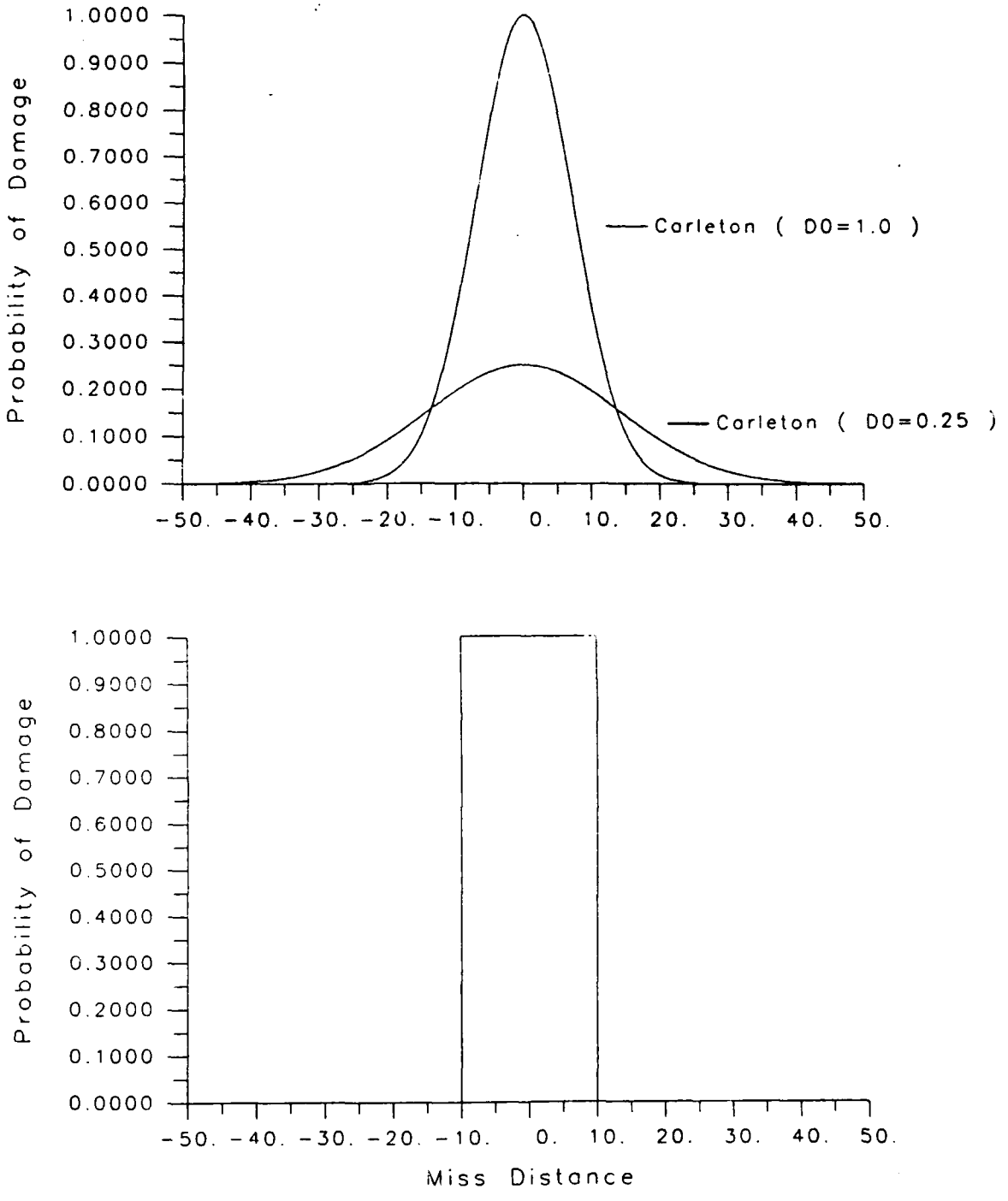

Figure 1: The Carleton (above) and Cookie Cutter Functions

II. Comparison of Carleton and Cookie Cutter Results

A. Single Aimpoint on Target

The purpose of this section is to prove that using a Cookie Cutter (CC) distribution to describe the vulnerability of a target to a single weapon will always produce a higher kill probability estimate than will using any other non-increasing function (such as the Carleton distribution[2]) if the target is at the aimpoint and the delivery system is un-biased. Furthermore, the probability of kill (Pk(K)) for any function, K, will approach that using a CC (Pk(CC)) as the impact distribution (which reflects the delivery errors) becomes uniform.

Before commencing, it is important to define the concept of lethal area, A_L. Mathematically, the lethal area of a weapon against a target at (u,v) is given by:

$$A_L = \int_{\infty} dA\, P_d(u, v, x, y) \tag{1}$$

where P_d is the probability of damage of a target at (u,v) due to a weapon at (x,y).

First, we present the three functions: the Cookie Cutter (CC), any other non-increasing damage function (K) and an impact distribution function P(r), which gives the probability of a warhead detonating at point r. Note: for simplicity in this presentation, we assume that all functions are circularly symmetrical. Thus, all functions will be written as functions of radius (r) only and all integrals will be expressed as

$$\int r\, dr$$

The three distributions (CC, K, P) have the following properties:

$$Cookie\ Cutter(CC) = \begin{cases} 1: & r \leq R \\ 0: & r > R \end{cases}$$

[2]The Carleton function is defined by:

$$P_d(u, v, x, y) = D_0\, e^{-D_0\left[\frac{(u-x)^2}{R_1^2} + \frac{(v-y)^2}{R_2^2}\right]}$$

where P_d is the probability of damage of a target at (u,v) due to a weapon at (x,y).

$$Other\ distribution\ (K) = \begin{cases} Continuous: & all\ r \\ Non-increasing: & all\ r \\ K(r) \leq 1: & all\ r \end{cases}$$

$$Impact\ distribution(P) = \begin{cases} Continuous: & all\ r \\ Non-increasing: & all\ r \\ 2\pi \int_0^\infty K(r)\, r\, dr = 1 & \end{cases}$$

Finally, since the CC and K distributions describe the same round, they must be normalized such that their lethal areas (A_L) are equal:

$$A_L(CC) = A_L(K) \tag{2}$$

where

$$A_L(CC) = 2\pi \int CC(r)\, r\, dr \tag{3}$$

$$A_L(K) = 2\pi \int K(r)\, r\, dr \tag{4}$$

For future convenience, we here point out that the integrals in equations 2 and 3 can be broken into a sum of integrals over intervals of arbitrary length δ as shown in equations 5 and 6.

$$A_L(CC) = 2\pi \sum_{r=0}^{R} \int_r^{r+\delta} CC(r)\, r\, dr \tag{5}$$

$$A_L(K) = 2\pi \sum_{r=0}^{\infty} \int_r^{r+\delta} K(r)\, r\, dr \tag{6}$$

Note: In equations 5 and 6, the summations are over values of r with step sizes = δ. Also, in equation 5, we observed that $CC(r) = 0\ for\ r > R$ and reduced the summation accordingly.

The probability of kill, Pk, for a single round versus a single target, is given by the probability of impacting at a given radius, P(r), times the probability of kill from a hit at that radius, (CC(r) or K(r)), integrated over all area.

$$Pk(CC) = 2\pi \int P(r)\, CC(r)\, r\, dr \tag{7}$$

$$Pk(K) = 2\pi \int P(r)\, K(r)\, r\, dr \tag{8}$$

The goal of this treatise is attained, therefore, by showing that

$$Pk(CC) \geq Pk(K) \tag{9}$$

The proof takes advantage of the fact that the probability function, P, is continuous. It is therefore always possible to find a step size δ such that

$$P(r) - P(r+\delta) \leq \epsilon$$

for any ϵ. We therefore can divide the integrals in equations 7 and 8 as follows:

$$Pk(CC) = 2\pi \sum_{r=0}^{R} P(r) \int_{r}^{r+\delta} CC(r)\, r\, dr \tag{10}$$

$$Pk(K) = 2\pi \sum_{r=0}^{\infty} P(r) \int_{r}^{r+\delta} K(r)\, r\, dr \tag{11}$$

$$Pk(K) = 2\pi \sum_{r=0}^{R} P(r) \int_{r}^{r+\delta} K(r)\, r\, dr + 2\pi \sum_{r=R}^{\infty} P(r) \int_{r}^{r+\delta} K(r)\, r\, dr \tag{12}$$

Notice that the summation in equation 10 stops at R since $CC(r) = 0$ for $r > R$. To stress the difference, equation 11 is broken into two summations in equation 12.

Now, we cleverly compare terms of equations 10 and 12 by grouping them as follows. For each term in the summation 0 to R in equation 10, there is a corresponding term in the first sum in equation 12. However, note that each such term from 12 is $\leq$ the corresponding term from 10 because $K(r) \leq 1$, and therefore the integral portion of the 12 term is $\leq$ the integral portion of the 10 term. Concentrating on the integral portions of the terms, we take from the SECOND sum in 12 as many terms or fractions of terms as are needed such that, when added to the FIRST sum integral, the total equals the 10 term integral. Mathematically,

$$\begin{aligned} P(r) \int_{r}^{r+\delta} CC(r)\, r\, dr \;\Rightarrow\; & P(r) \int_{r}^{r+\delta} K(r)\, r\, dr + P(s) \int_{s}^{s+\delta} K(r)\, r\, dr \\ & + P(t) \int_{t}^{t+\delta} K(r)\, r\, dr + \cdots \end{aligned} \tag{13}$$

such that

$$\int_r^{r+\delta} CC(r) r\, dr = \int_r^{r+\delta} K(r) r\, dr + \int_s^{s+\delta} K(r) r\, dr + \int_t^{t+\delta} K(r) r\, dr + \cdots \quad (14)$$

This mapping is shown in Figure 2.

We now note that the left hand side of equation 14 is one of the terms of equation 5. Thus, in conducting the mapping over all terms from r = 0 to r = R, the sum of the left-hand terms will equal A_L. However, by equation 6, the right hand terms of equation 14 will equal A_L if summed over all such terms. Thus, by equation 1, we conclude that the above mapping exhausts all terms in equation 12.

Finally, we note that each term in equation 13 is of the form:

$$P(r)\, a \Rightarrow P(r)\, b + P(s)\, c + P(t)\, d + \cdots$$

where $a = b + c + d + \cdots$. However, P(r) is $\geq$ P(s), P(t), ... , and thus:

$$P(r)\, a \geq P(r)\, b + P(s)\, c + P(t)\, d + \cdots$$

Applying this to equation 7, we have:

$$\begin{aligned} P(r) \int_r^{r+\delta} CC(r)\, r\, dr \;\geq\; & P(r) \int_r^{r+\delta} K(r)\, r\, dr + P(s) \int_s^{s+\delta} K(r)\, r\, dr \\ & + P(t) \int_t^{t+\delta} K(r)\, r\, dr + \cdots \end{aligned} \quad (15)$$

If we now sum equation 15 over all terms in the mapping, the left hand side sums to equation 10 and, since the mapping exhausts all terms, the right-hand side sums to equation 12. We have therefore proven equation 9, as required.

We now consider the behavior of this relationship at the extrema.

1. As P(r) approaches a constant, the left- and right-hand sides of equation 15 become strictly equal. Therefore, Pk(CC) $\Rightarrow$ Pk(K). (This can also be easily seen by substituting P(r) = p into equations 7 and 8 and comparing with equations 2 and 3.)

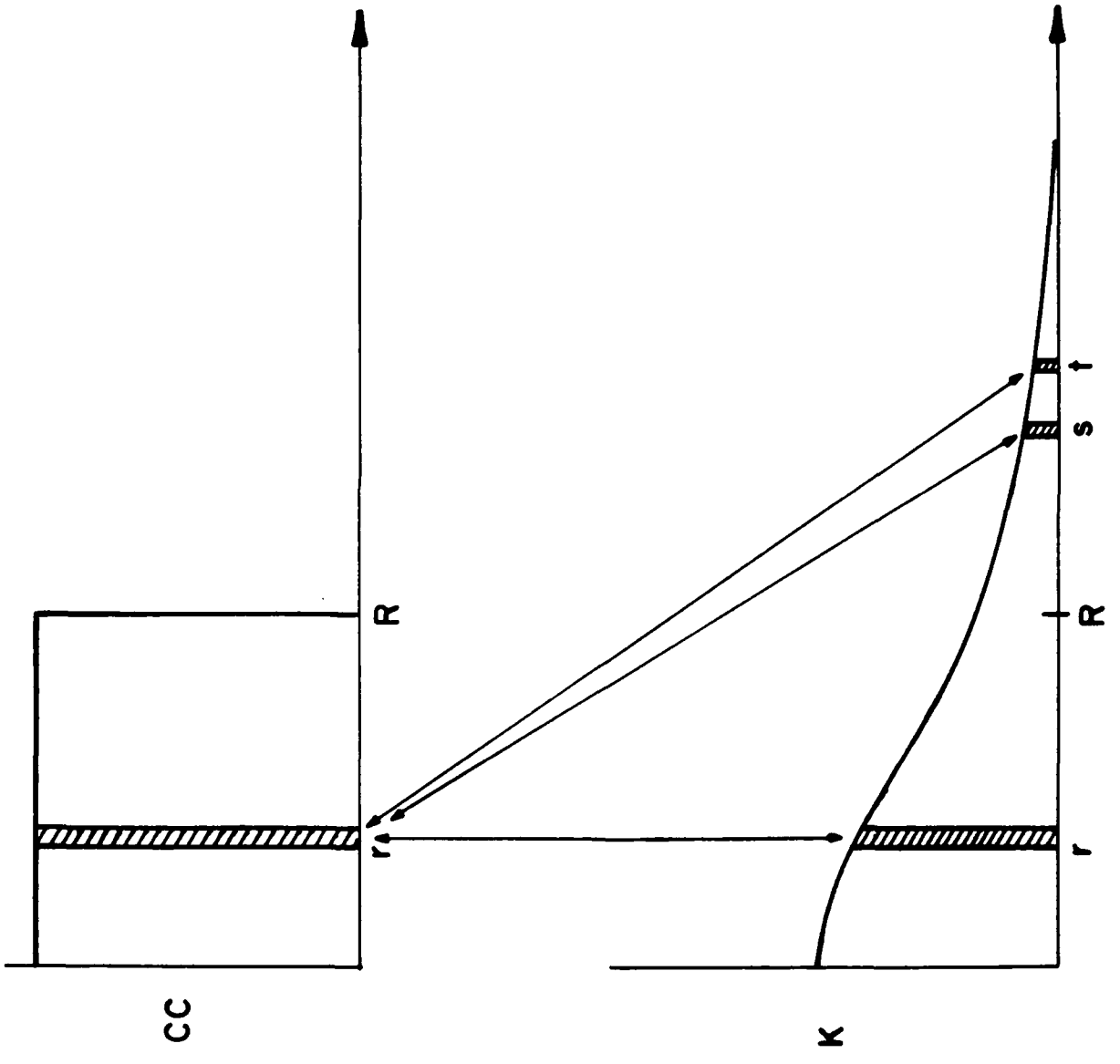

Figure 2: Mapping of Pk(Cookie Cutter) onto Pk(Other)

2. As P(r) approaches a delta function (at 0, of course, in keeping with property #2), all terms in equation 15 go to 0 except the first (at r = 0). We then have:

   - Pk(CC) $\Rightarrow \int_0^\delta P(0)\, r\, dr = 1.$
   - Pk(K) $\Rightarrow \int_0^\delta P(0)\, K(0)\, r\, dr = K(0)$

Thus, Pk(CC) and Pk(K) converge for inaccurate weapons; however, for accurate weapons, since K(0) is customarily significantly less than 1, Pk(CC) exceeds Pk(K). (A "rule-of-thumb" often used is to set K(0) = 0.25.)

As a numerical example of the above theorem, a comparison was made, over a wide range, of the predicted values of Pk for a Cookie Cutter of radius R and a Carleton-like function of the form:

$$K(r) = K(0)\, e^{-r^2/s^2}$$

A Gaussian probability function was used of the form:

$$P(r) = \frac{1}{\pi\, \sigma^2}\, e^{-r^2/\sigma^2}$$

Performing the integrals prescribed in equations 7 and 8, we get:

$$Pk(CC) = 1 - e^{-R^2/\sigma^2}$$

and

$$Pk(K) = s^2/(\sigma^2 + s^2)$$

Similarly, equations 2 and 3 yield

$$A_L(CC) = 2\pi \int CC(r)\, r\, dr = \pi\, R^2$$

$$A_L(K) = 2\pi \int K(r)\, r\, dr = \pi\, K(0)\, s^2$$

Since R and s are chosen to make $A_L(CC) = A_L(K)$, we can solve for s in terms of R and K(0) and substitute into the equation for Pk(K). Forming the ratio of Pk(CC) / Pk(K) and setting $R^2/\sigma^2 = q$, we have

$$\frac{Pk(CC)}{Pk(K)} = \frac{1 - e^{-q}}{\frac{K(0)q}{K(0)+q}}$$

A simple computer routine was written to evaluate the above ratio. Results are listed in Table 1 for two choices of K(0): 0.25 and 1.

As can be seen, the numerical example obeys the extrema behavior predicted above: For $R^2/\sigma^2 = q \rightarrow 0$, the ratio of Pk(CC)/Pk(K) goes to 1. This corresponds to an inaccurate weapon. On the other hand, for $R^2/\sigma^2 = q \rightarrow \infty$, (an extremely accurate weapon), the ratio goes to 1 / K(0).

B. Single Aimpoint off Target

If the mean aimpoint of the incoming weapon does not coincide with the location of the target, the "non-decreasing" requirement of the impact distribution no longer holds and thus the proof presented above can not be applied. In fact, it is obvious that a weapon accurately fired at a point outside of the Cookie Cutter radius from the target will have no probability of causing damage: In that situation, the Cookie Cutter will always predict less damage than the Carleton, whose infinite "tails" always show a non-zero probability of damage.

In this section, the results from a series of numerical studies are reported to demonstrate the different behavior of the CC and Carleton damage functions as a function of fixed aiming biases and delivery errors. For this study, the MCARTEF Code, reported in a following section, was used.

For these studies, three damage functions were chosen. The parameters of the functions are shown in Table 2.

Note that the lethal area of all damage functions was identical (314.15 m^2, corresponding to a Cookie Cutter radius of 10 m.). Since lethal area is commonly used as the primary measure of weapon performance, it is appropriate to treat these damage functions as describing equivalent weapons and thus compare their results.

Table 1: Numerical simulation of Pk(CC) / Pk(K)

q	$\frac{Pk(CC)}{Pk(K)}$,K(0)=0.25	$\frac{Pk(CC)}{Pk(K)}$,K(0)=1.
1.0E-4	1.001	1.000
3.0E-4	1.001	1.000
1.0E-3	1.003	1.000
3.0E-3	1.011	1.002
1.0E-2	1.035	1.005
3.0E-2	1.109	1.015
1.0E-1	1.332	1.047
0.126	1.413	1.058
0.158	1.511	1.071
0.200	1.630	1.087
0.251	1.772	1.106
0.316	1.942	1.128
0.398	2.139	1.153
0.501	2.363	1.181
0.631	2.613	1.210
0.794	2.882	1.238
1.000	3.161	1.264
1.259	3.433	1.285
1.585	3.682	1.297
1.995	3.889	1.297
2.512	4.041	1.285
3.162	4.134	1.261
3.981	4.172	1.228
5.012	4.172	1.192
6.310	4.151	1.156
7.943	4.124	1.125
1.0E1	4.100	1.100
3.0E1	4.032	1.032
1.0E2	4.010	1.010
3.0E2	4.003	1.003
1.0E3	4.001	1.001
3.0E3	4.000	1.000
1.0E4	4.000	1.000
3.0E4	4.000	1.000
1.0E5	4.000	1.000

Table 2: Damage Function Parameters

Type	A_L	Pk(0) or D_0
Carleton	314.159	0.25
Carleton	314.159	1.0
Cookie Cutter	314.159	1.0

A series of target points were set up along a line at the following distances from the origin (x = 0).

$$x = 0, 2, 4, 7, 10, 15, 20, 35, 50$$

At each target point, three targets were placed, one associated with each of the damage functions. All rounds were aimed at the x=0 point. Thus, analysis of a study (a Monte Carlo sampling of 5000 rounds) gives a complete set of results for all three damage functions and for all aimpoint biases given by the above list.

The study was repeated nine times, each time choosing a different set of delivery errors. Since each attack (of the 5000 in each study) consisted only of one round, there was no difference between mean-point-of-impact (MPI) and round-to-round errors; we chose to input the errors into MCARTEF as round-to-round errors. However, note that the errors were input (equally) in both the range and deflection dimensions. The values chosen for the delivery errors coincided with thoses chosen for the biases, viz:

$$x = 0, 2, 4, 7, 10, 15, 20, 35, 50$$

The results from the nine studies were then reaggregated, by aimpoint bias, and plotted versus delivery error. These results are presented in Figures 3 through 11.

It is of general interest to note some of the salient features of the results. As expected for low biases (proven above for bias = 0), the Cookie Cutter produces a higher probability of damage than either Carleton.

Once the bias exceeds the Cookie Cutter radius, we see a reversal: the low D_0 Carleton has the higher damage probability for low delivery errors. Interestingly, there is a cross-over, even for very large biases: as the delivery error is increased, the Cookie Cutter (and high D_0 Carleton) again become the bigger damage probability functions.

We also notice the expected decrease in damage probability with increasing bias. (Note the scale change for the higher biases.) Note also the extent

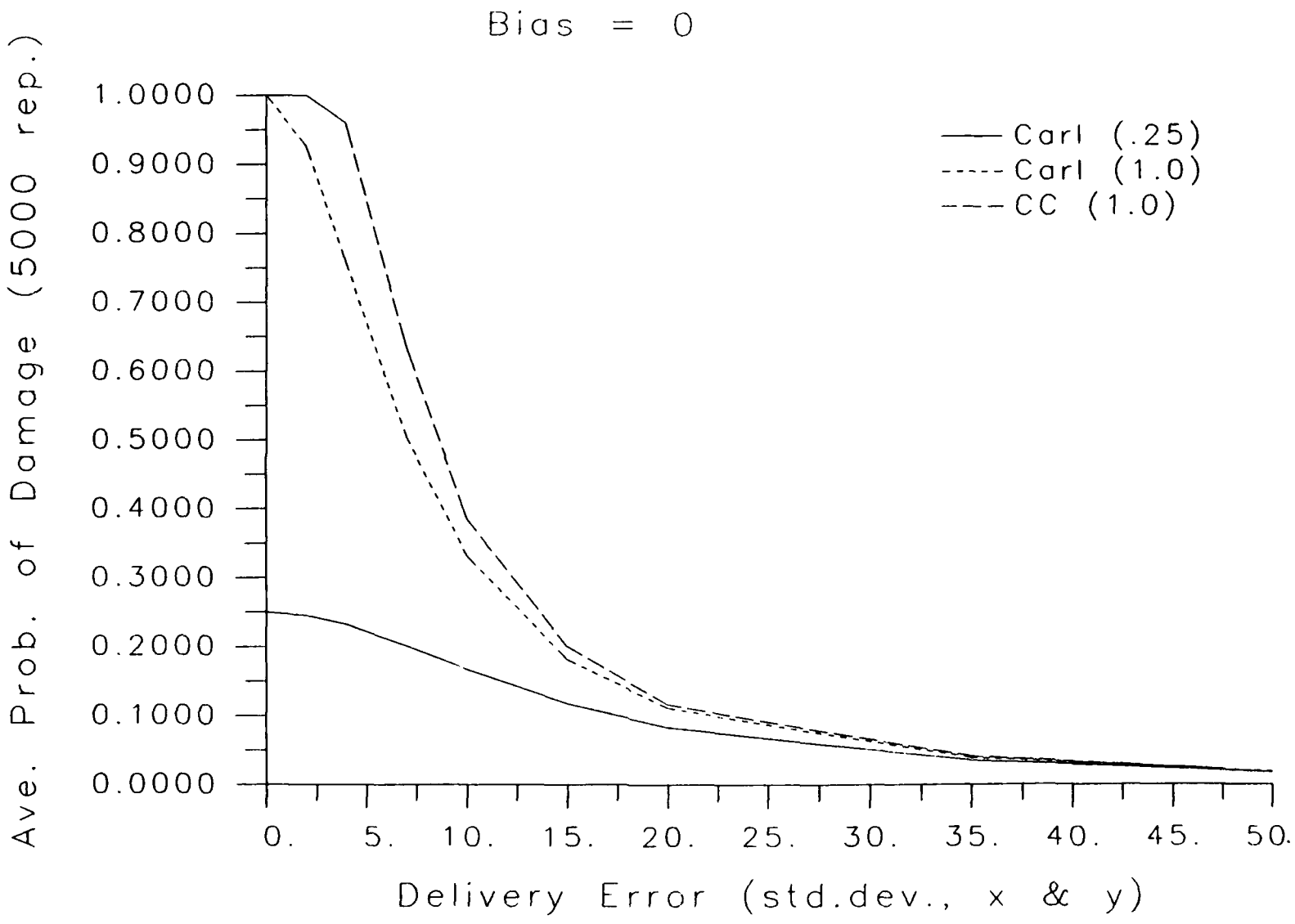

Figure 3: Comparison of CC and Carleton Results for Aimpoint Bias = 0

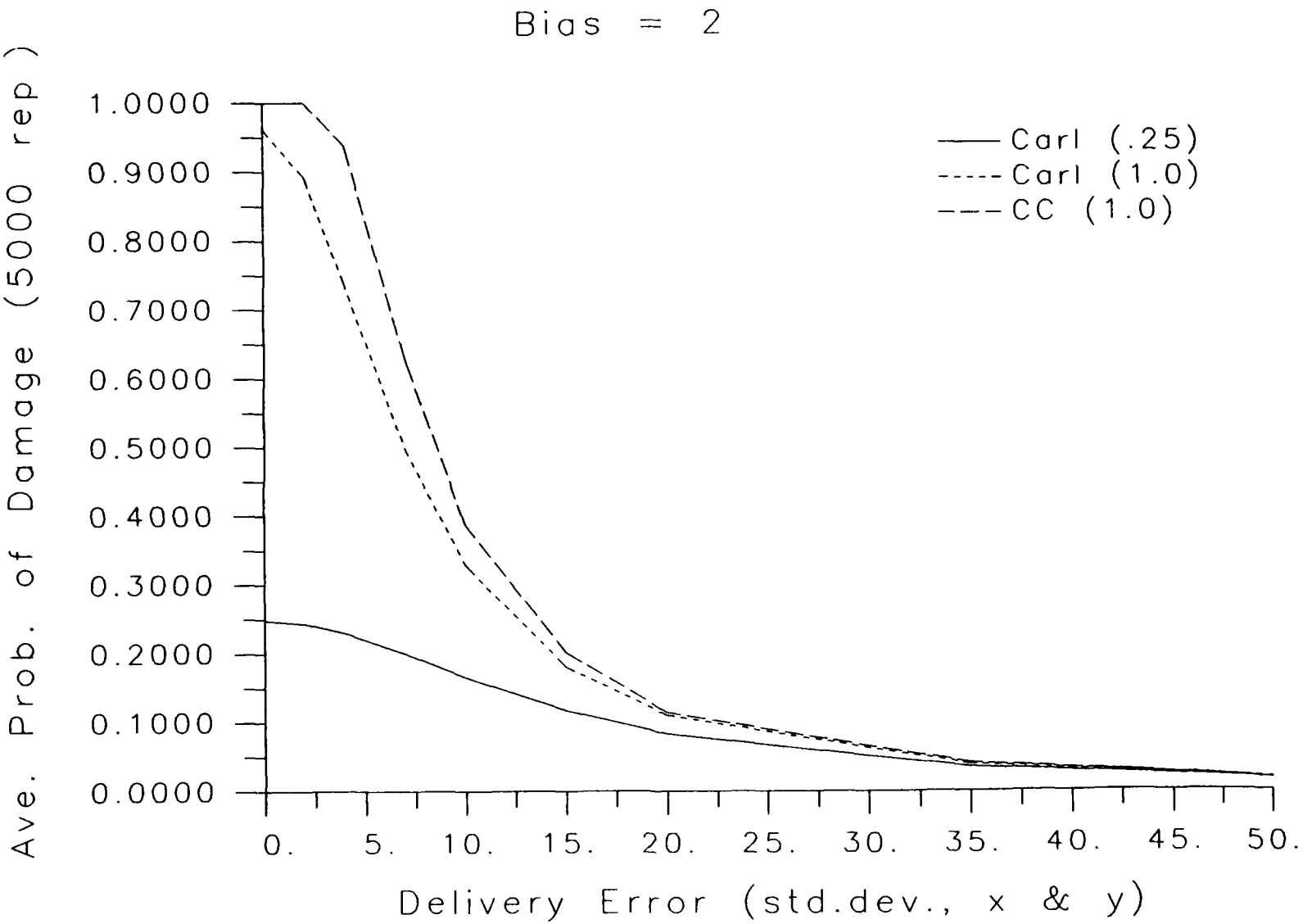

Figure 4: Comparison of CC and Carleton Results for Aimpoint Bias = 2

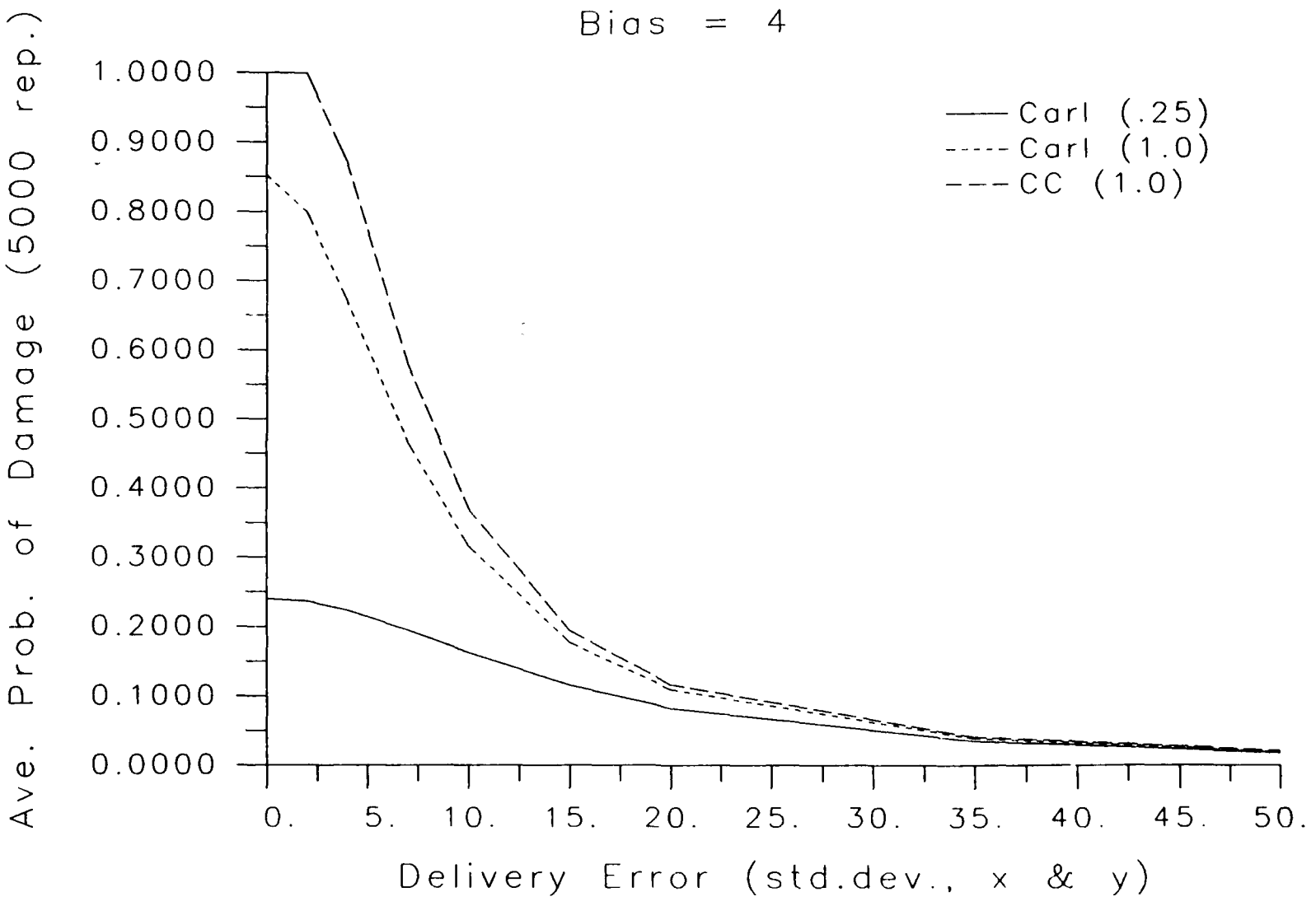

Figure 5: Comparison of CC and Carleton Results for Aimpoint Bias = 4

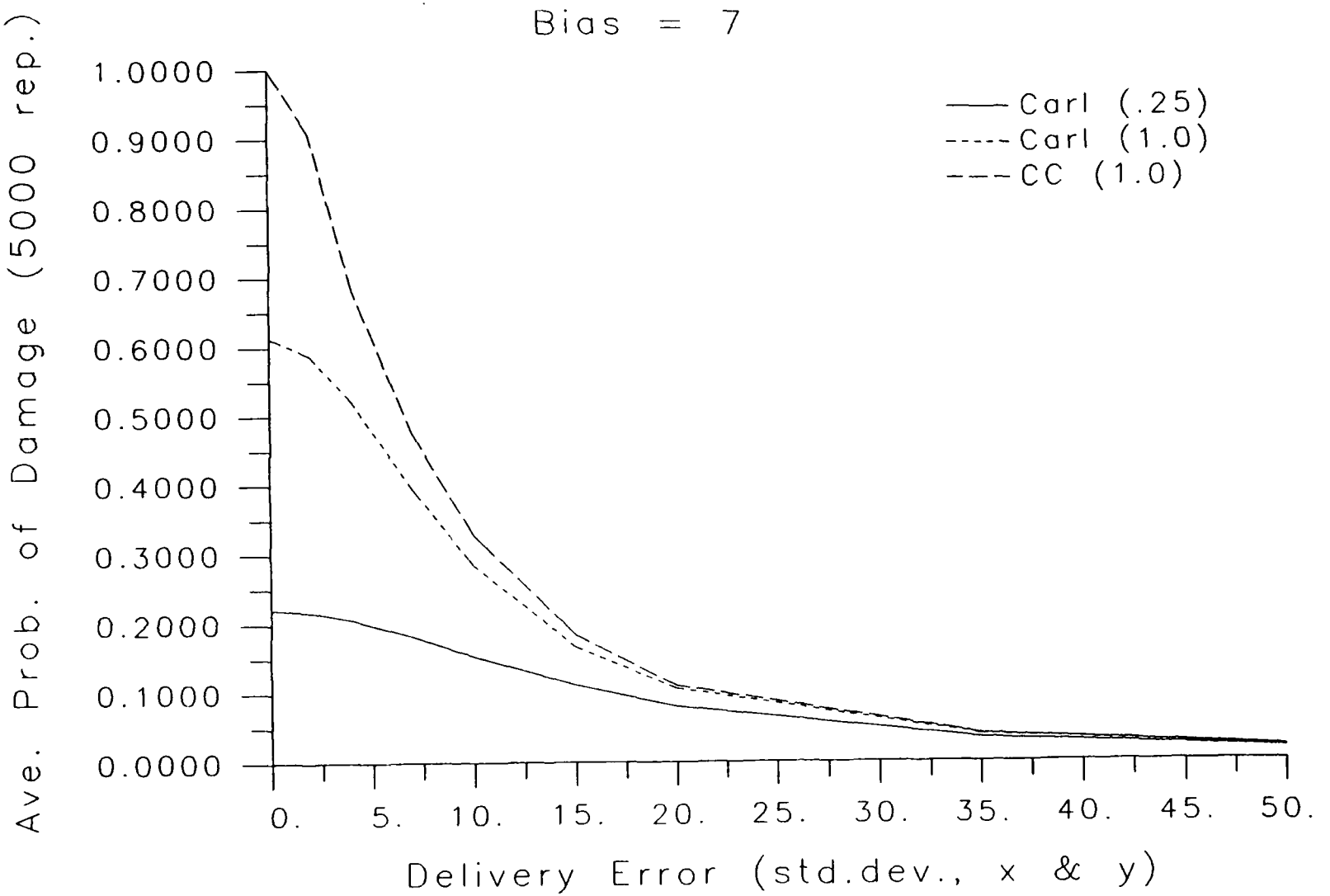

Figure 6: Comparison of CC and Carleton Results for Aimpoint Bias = 7

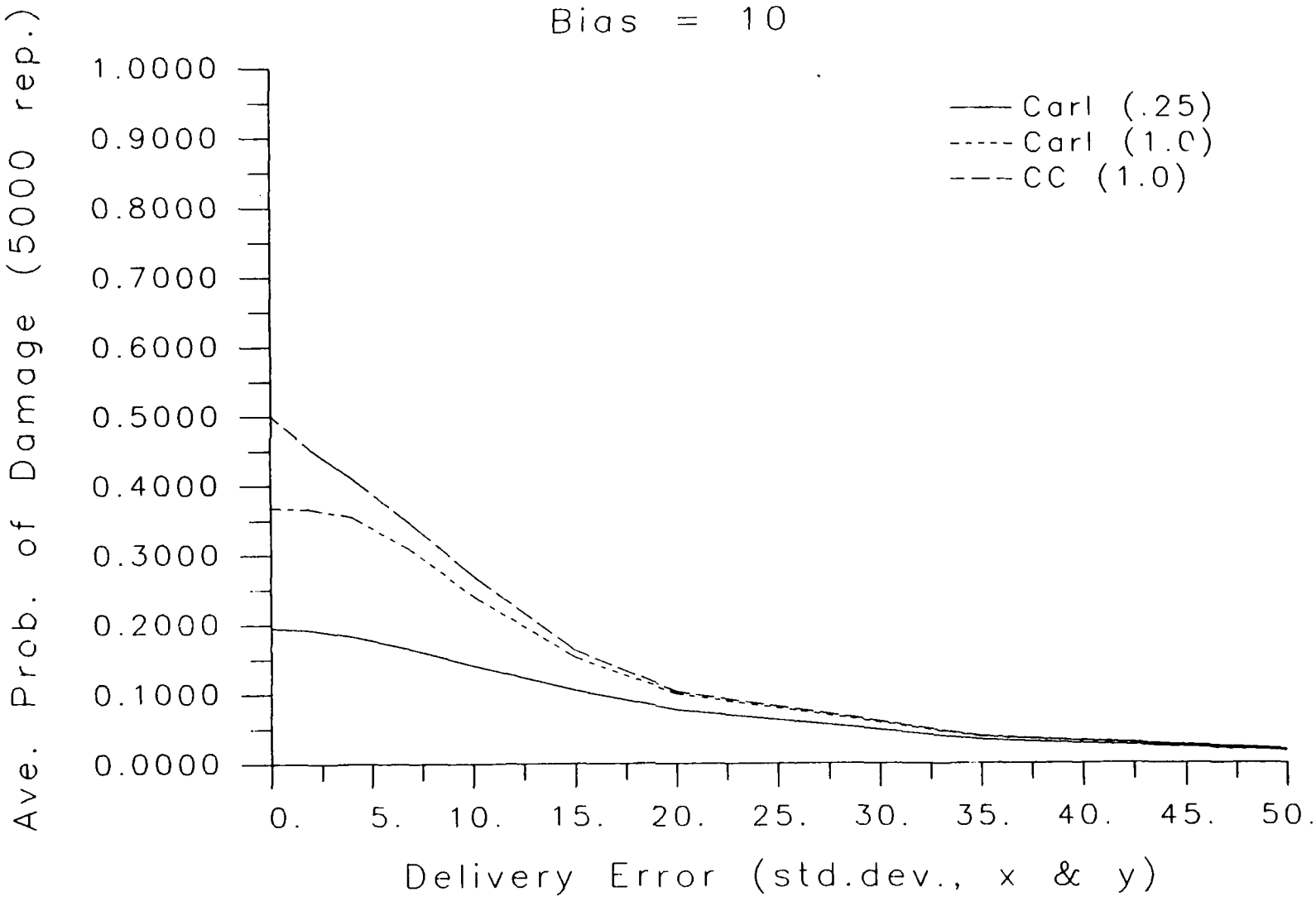

Figure 7: Comparison of CC and Carleton Results for Aimpoint Bias = 10

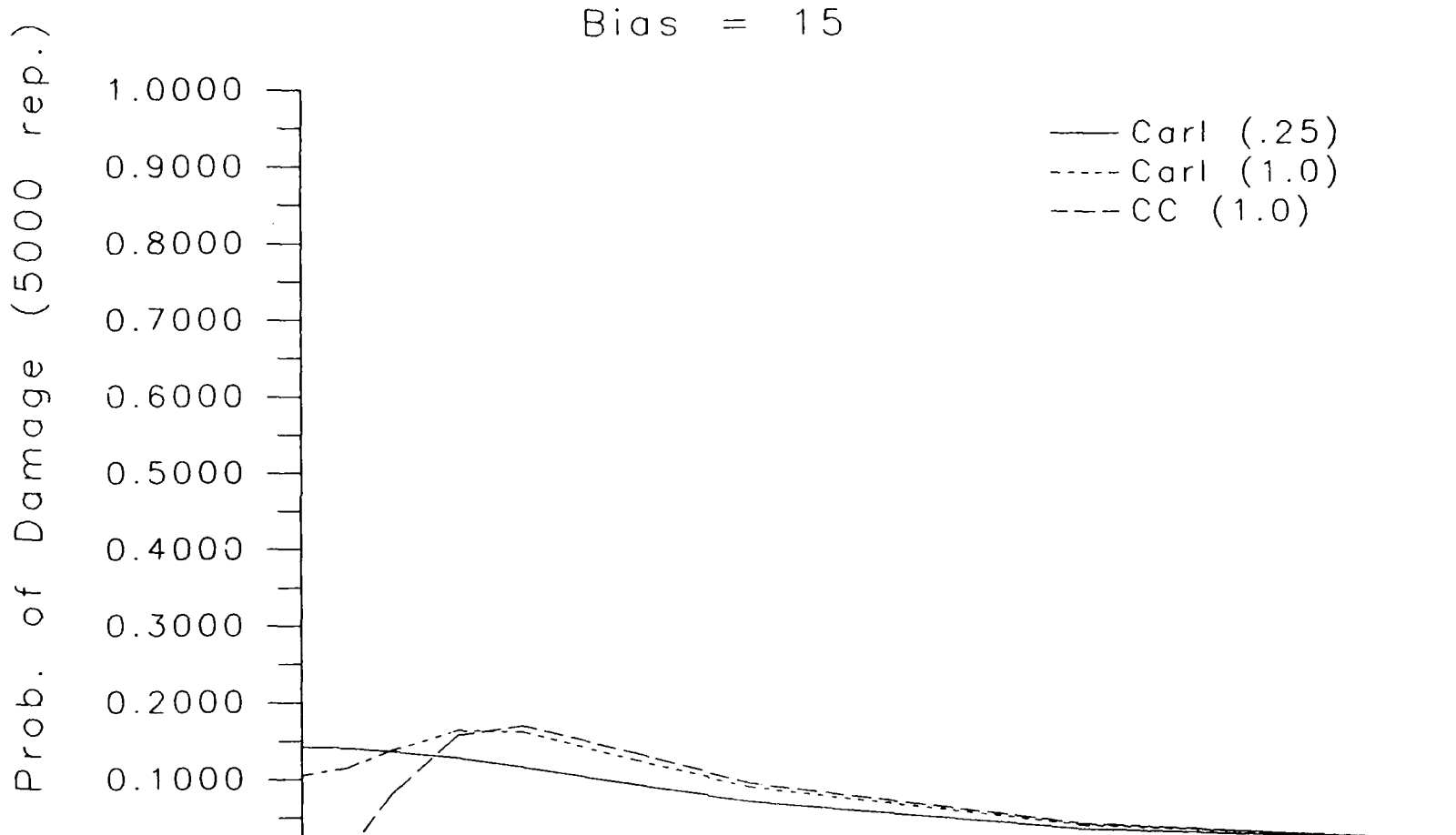

Figure 8: Comparison of CC and Carleton Results for Aimpoint Bias = 15

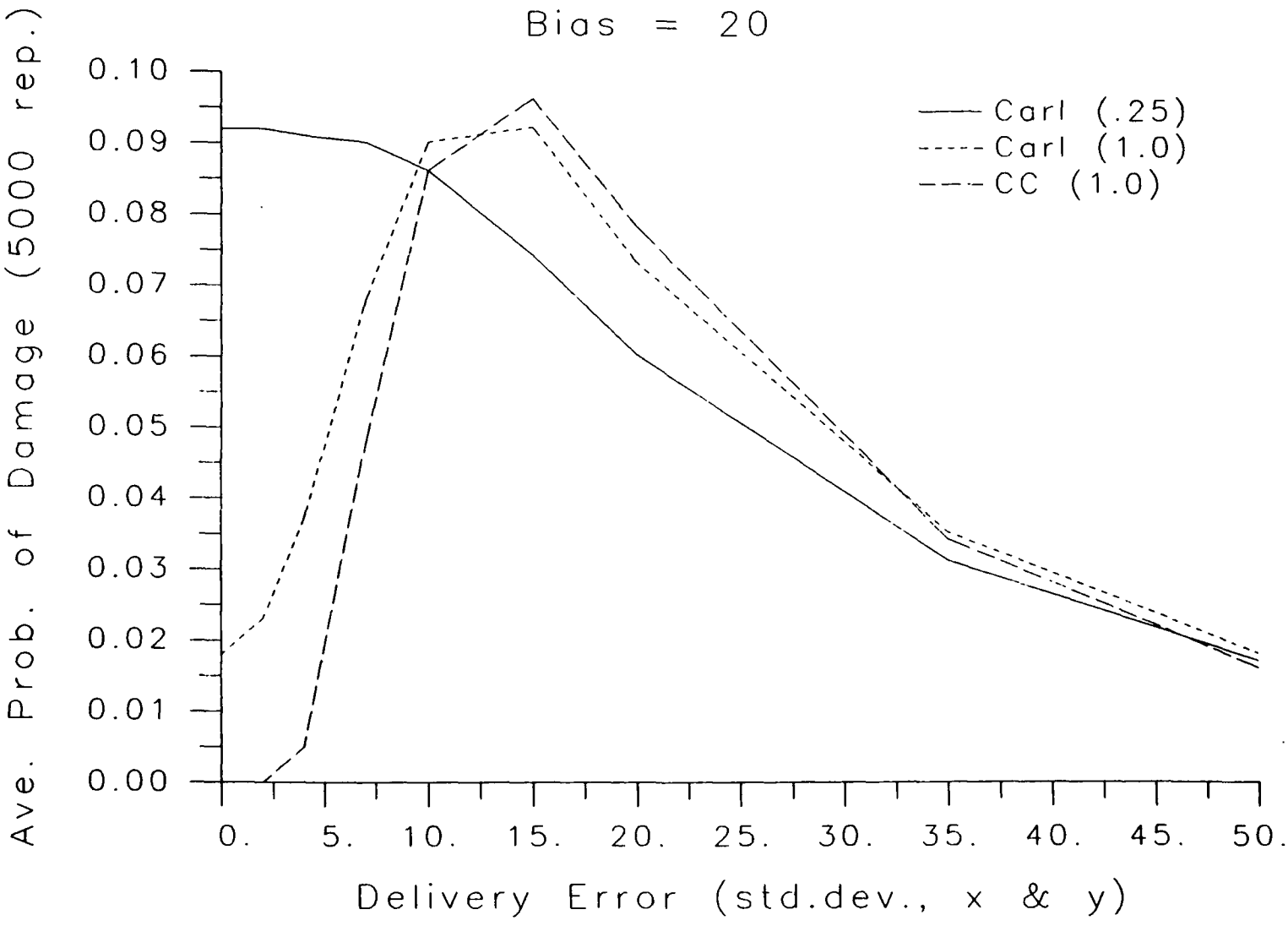

Figure 9: Comparison of CC and Carleton Results for Aimpoint Bias = 20

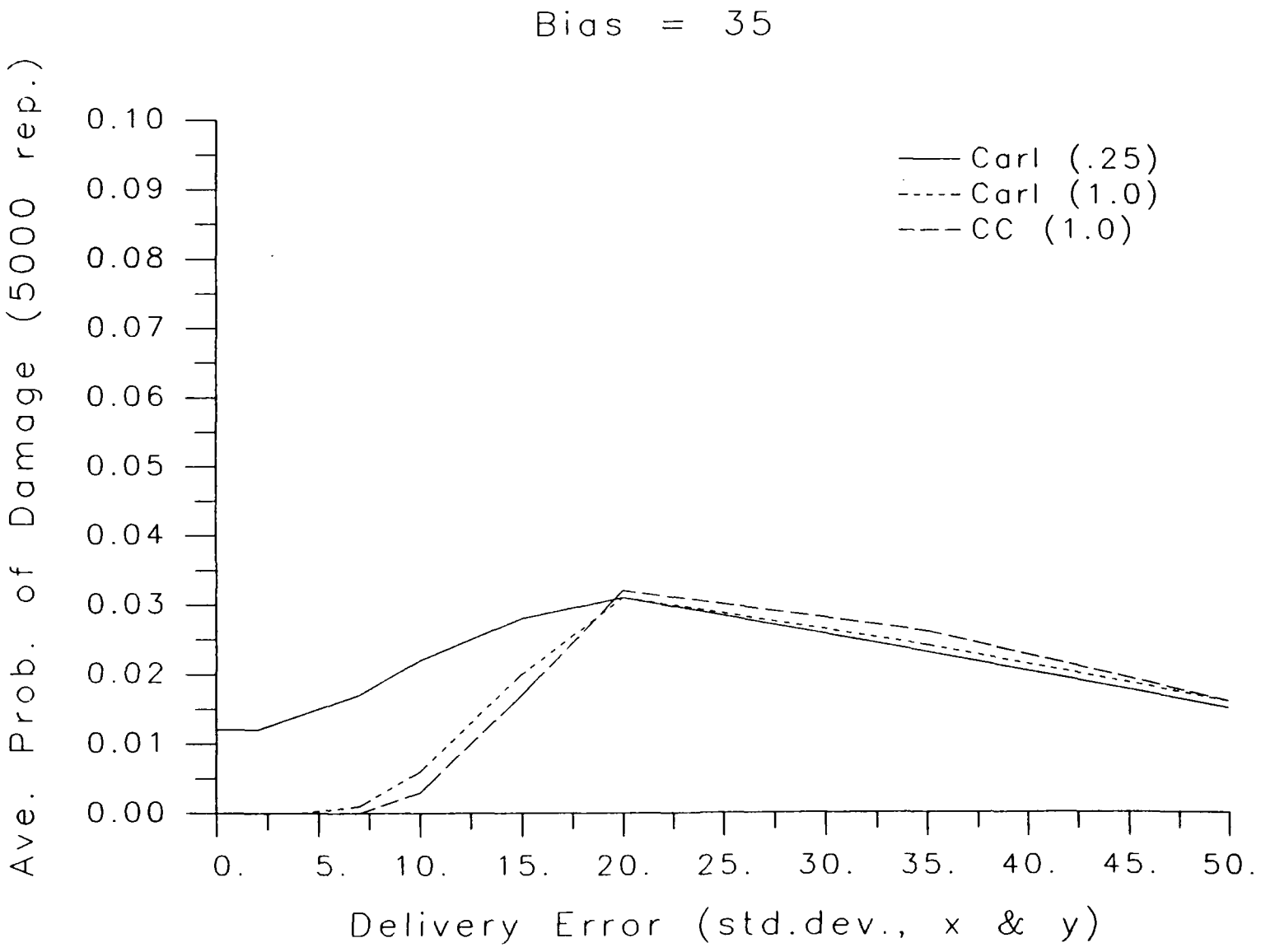

Figure 10: Comparison of CC and Carleton Results for Aimpoint Bias = 35

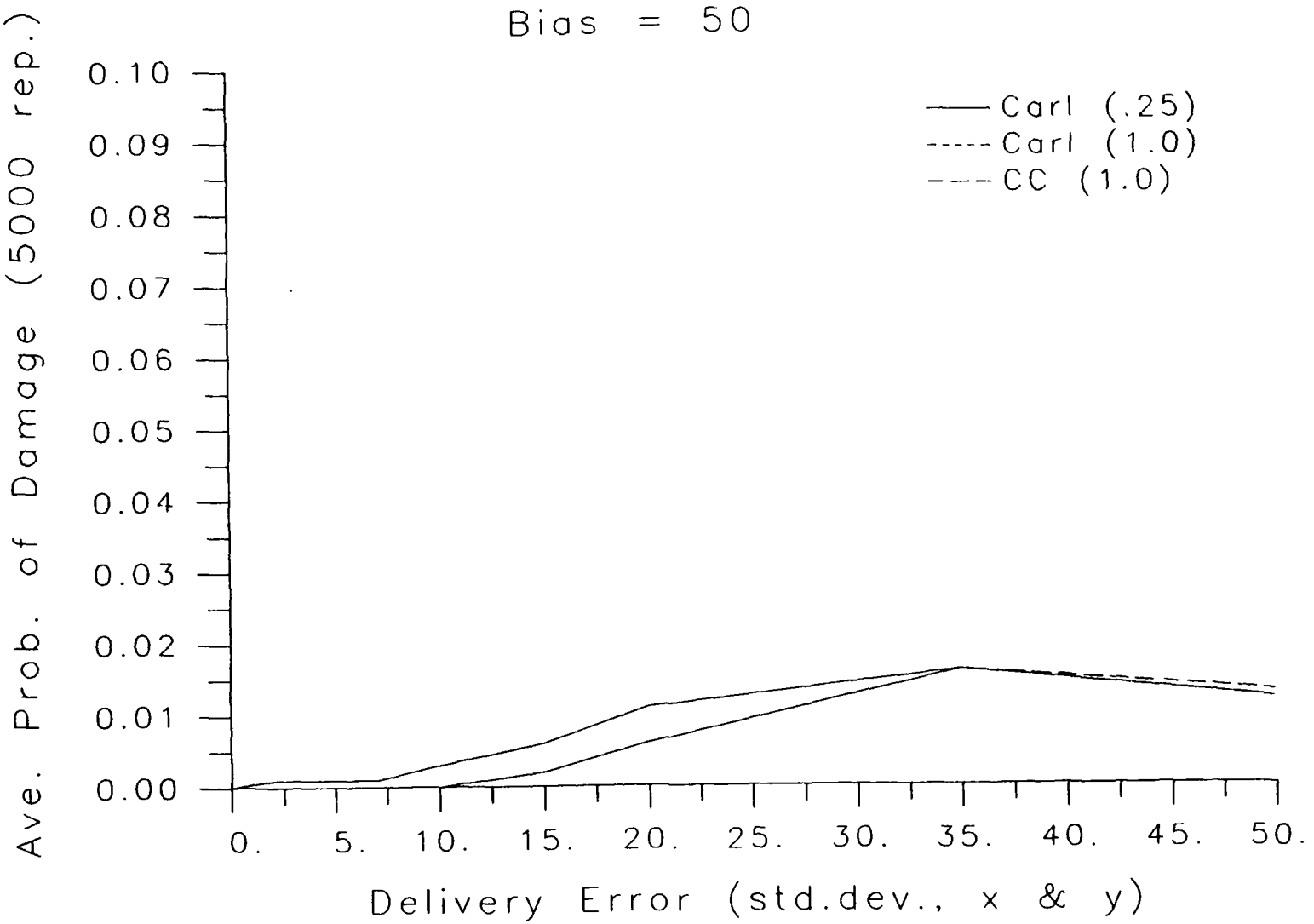

Figure 11: Comparison of CC and Carleton Results for Aimpoint Bias = 50

to which the probability of damage increases with increasing delivery error. In this case, the delivery error serves the same function as the spread in a multi-round pattern.

III. The Hybrid (Klopcic) Function

A. Function Definition

The Carleton and Cookie Cutter functions discussed above have certain significant shortcomings that make each of them disadvantageous for use as damage functions for conventional area weapons (e.g., fragmenting artillery rounds and bombs).

The Carleton: Significantly underevaluates kills from direct hits and near misses - especially when D_0 (see footnote 2) is set substantially less than 1, which is commonly done for artillery.

The Cookie Cutter: Over-estimates the size of the direct-hit/near-miss area and ignores the possibility of kills from distant misses.

On the other hand, the functions have certain very good characteristics, viz:

1. Both preserve the lethal area of the warhead being modeled.
2. Both allow for range-deflection asymmetry in the effects.
3. Both are integrable in closed form, allowing easy normalization (to the lethal area).
4. Both are continuous: the Carleton is continuous in all its derivatives.

The goal of the section is to present a function that relieves the above shortcomings while preserving the good characteristics of the CC and Carleton functions.

The function so derived, herein referred to as the Klopcic function, is a hybrid combination of the Cookie Cutter and Carleton functions. Mathematically, the Klopcic function can be expressed as:

$$Klopcic\,Function\,(KL) = \begin{cases} Pk_0 : & \frac{x^2}{A^2} + \frac{y^2}{B^2} \leq 1. \\ Pk_0\, e^{-[u^2/\sigma_x^2 + v^2/\sigma_y^2]} : & elsewhere \end{cases} \qquad (16)$$

where:

$$Pk_0, A, B, \sigma_x, \sigma_y = \text{parameters of the distribution} \quad (17)$$

$$\frac{A}{B} = \frac{\sigma_x}{\sigma_y} \quad (18)$$

$$u = x - x_0 \quad (19)$$

$$v = y - y_0 \quad (20)$$

$$\frac{x_0^2}{A^2} + \frac{y_0^2}{B^2} = 1. \quad (21)$$

$$\frac{x_0}{y_0} = \frac{x}{y} \quad (22)$$

A cross-sectional plot of the function is shown in Figure 12.

It is shown in Appendix A that the lethal area for the Klopcic function can be expressed as:

$$A_L(KL) = \pi\, Pk_0\, A\, B + \frac{\pi\, A\, Pk_0}{B}\left[\sigma_y^2 + B\,\sigma_y\,\sqrt{\pi}\right] \quad (23)$$

These factors can be used to simplify parameter input for the Klopcic function. Referring to Figure 12, we note that a salient feature of the Klopcic function is the flat-topped core, which extends to $\pm A$ in the x direction and to $\pm B$ in the y direction. The damage probability in this region is a constant, denoted by Pk_0. The lethal area in this region, A_{L0}, is thus given by

$$A_{L0} = \pi\, A\, B\, Pk_0 \quad (24)$$

Another distinguishing feature of the Klopcic function, which does not show in Figure 12, is the eccentricity of the function in x-y, given by the ratio of A to B:

$$rat = \frac{A}{B} \quad (25)$$

Note: As specified in equation 18, the eccentricity is common for both the central flat-top and the surrounding tails.

With these relationships, it is possible to define the parameters for a Klopcic function in terms that are physically meaningful for the user:

A_L: the total lethal area of the weapon against the target, as defined in equation 23.

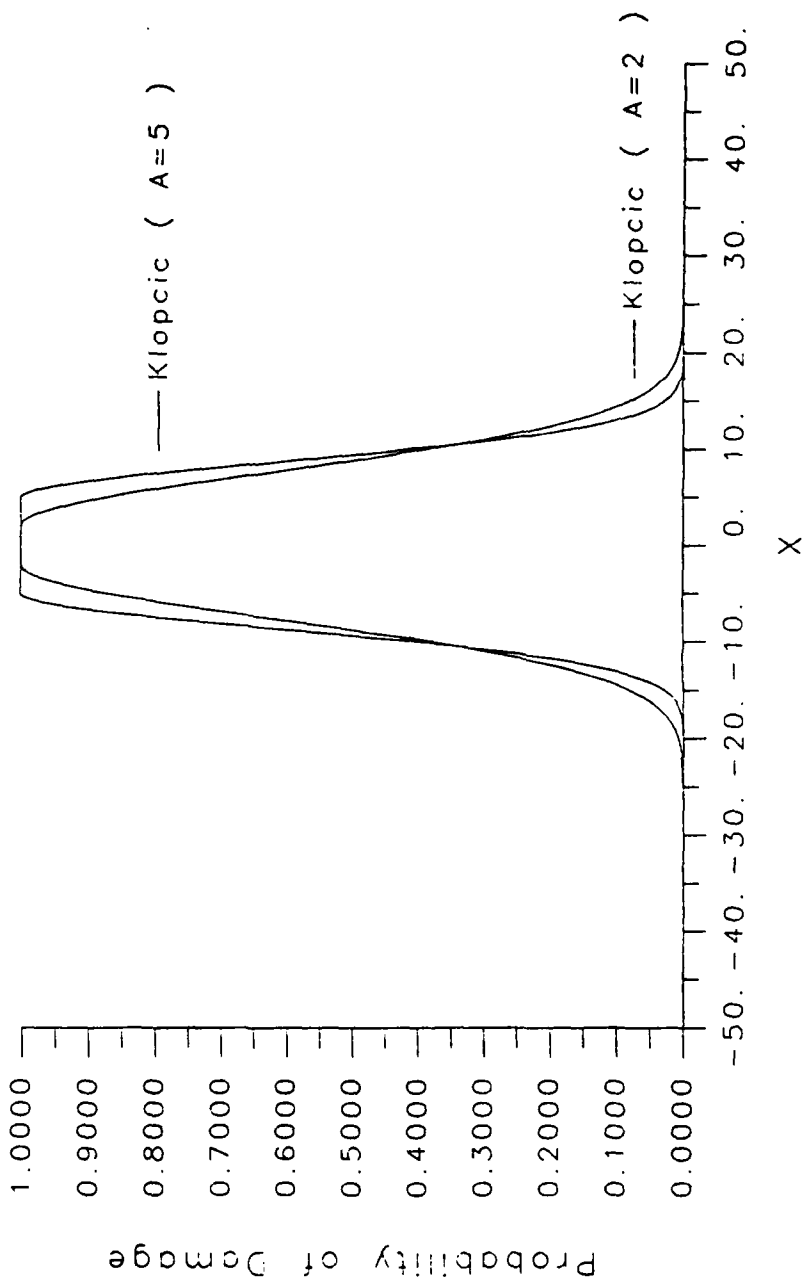

Figure 12: The Klopcic Function

rat: A/B, the ratio of x and y extents of the central region.

Pk_0: the probability of damage in the central region.

A_{LO}: the lethal area of the central core.

It is seen that the first three of the input parameters are defined precisely as they are defined for the traditional Cookie Cutter and Carleton functions. The fourth parameter, A_{LO}, represents the area of the direct hit/near-miss region multiplied by the probability of damage in that region. The Klopcic function therefore provides an intuitively appealing way to include direct hits into a damage function for a fragmenting munition.

B. Single Aimpoint off Target

In order to get a better appreciation of the behavior of the Klopcic damage function, the series of numerical studies described in section II.B. were repeated, this time comparing the Cookie Cutter, the Carleton with $D_0 = 0.25$, and two examples of the Klopcic function. The two Klopcic functions corresponded to central (direct hit/near miss) radii of 5 and 2 meters. In comparison, the Cookie Cutter radius was 10 meters.

As in section II.B., the results (probabilities of damage) are plotted versus delivery errors for each of the nine fixed aiming biases. These are presented in Figures 13 through 21. Again, the MCARTEF Code was used.

As anticipated, the results for both of the Klopcic functions lay between the Cookie Cutter and the Carleton results. For low biases and low delivery errors (high probability of a direct hit), the Klopcic function results closely approximate the CC results. As delivery errors increase, all results converge toward a zero asymptote.

The behavior of the results with increasing bias errors is quite interesting. The CC is only minimally affected by small changes in bias error. However, as the bias error approaches the CC radius, the CC results plunge precipitously until, at biases just larger than the CC radius, the cross-over described in section II.B. takes place. In all cases, the Klopcic function results remain bracketed by the Carleton and CC results. That is, while the CC values are larger than the Carleton's, the Klopcic values are smaller than the CC's; however, after reversal, the Klopcic values are larger than the CC values.

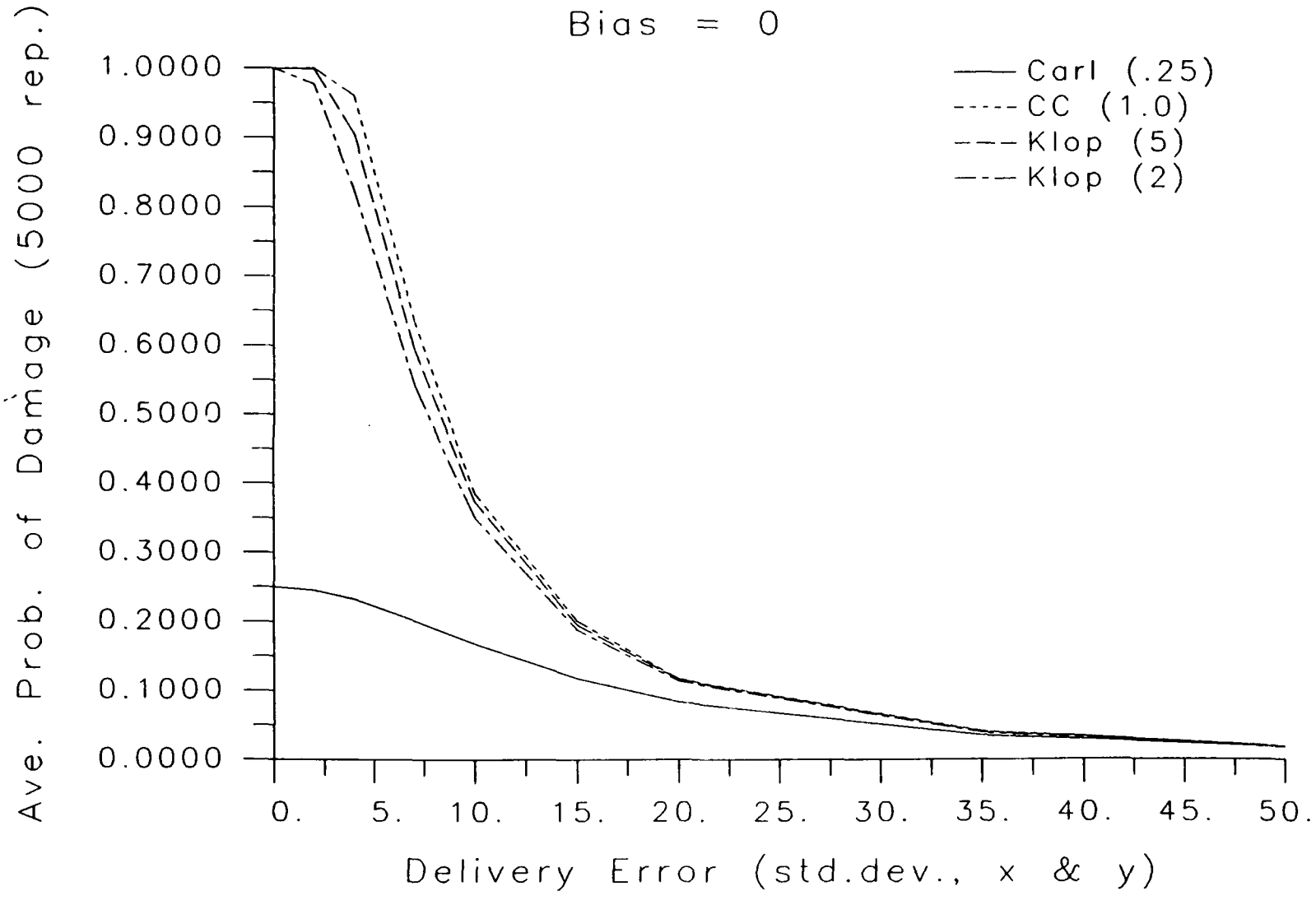

Figure 13: Klopcic, CC and Carleton Results for Aimpoint Bias = 0

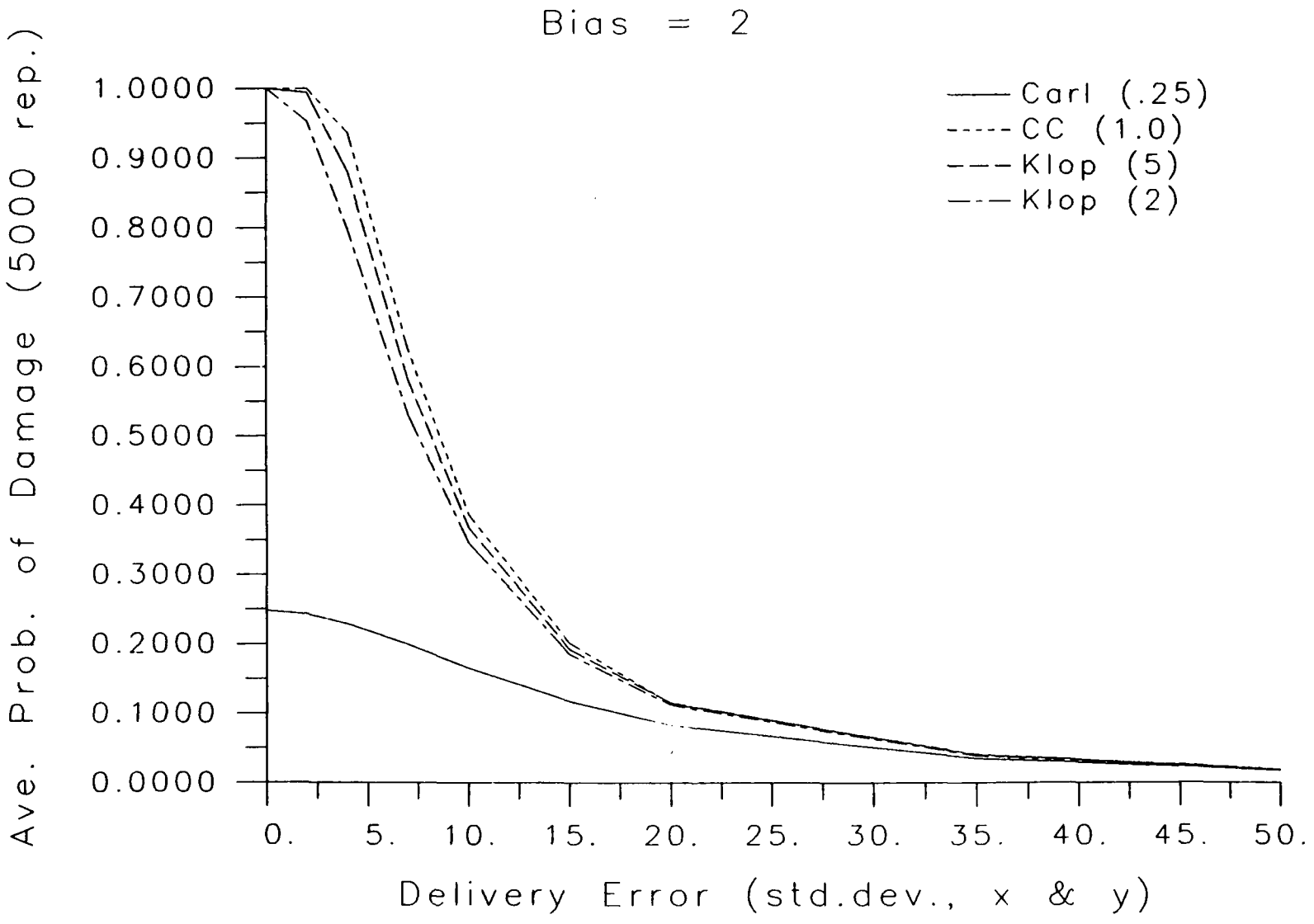

Figure 14: Klopcic, CC and Carleton Results for Aimpoint Bias = 2

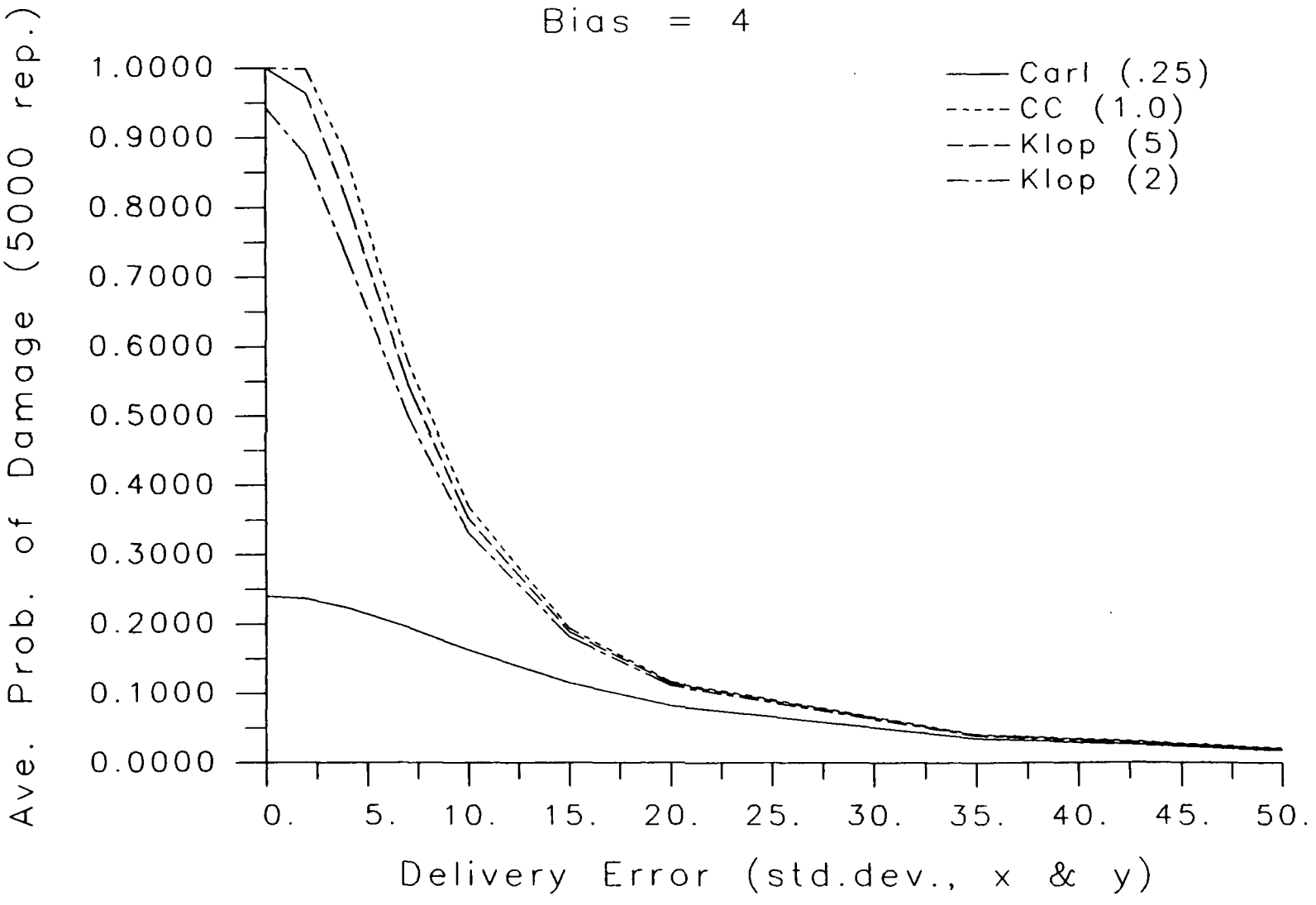

Figure 15: Klopcic, CC and Carleton Results for Aimpoint Bias = 4

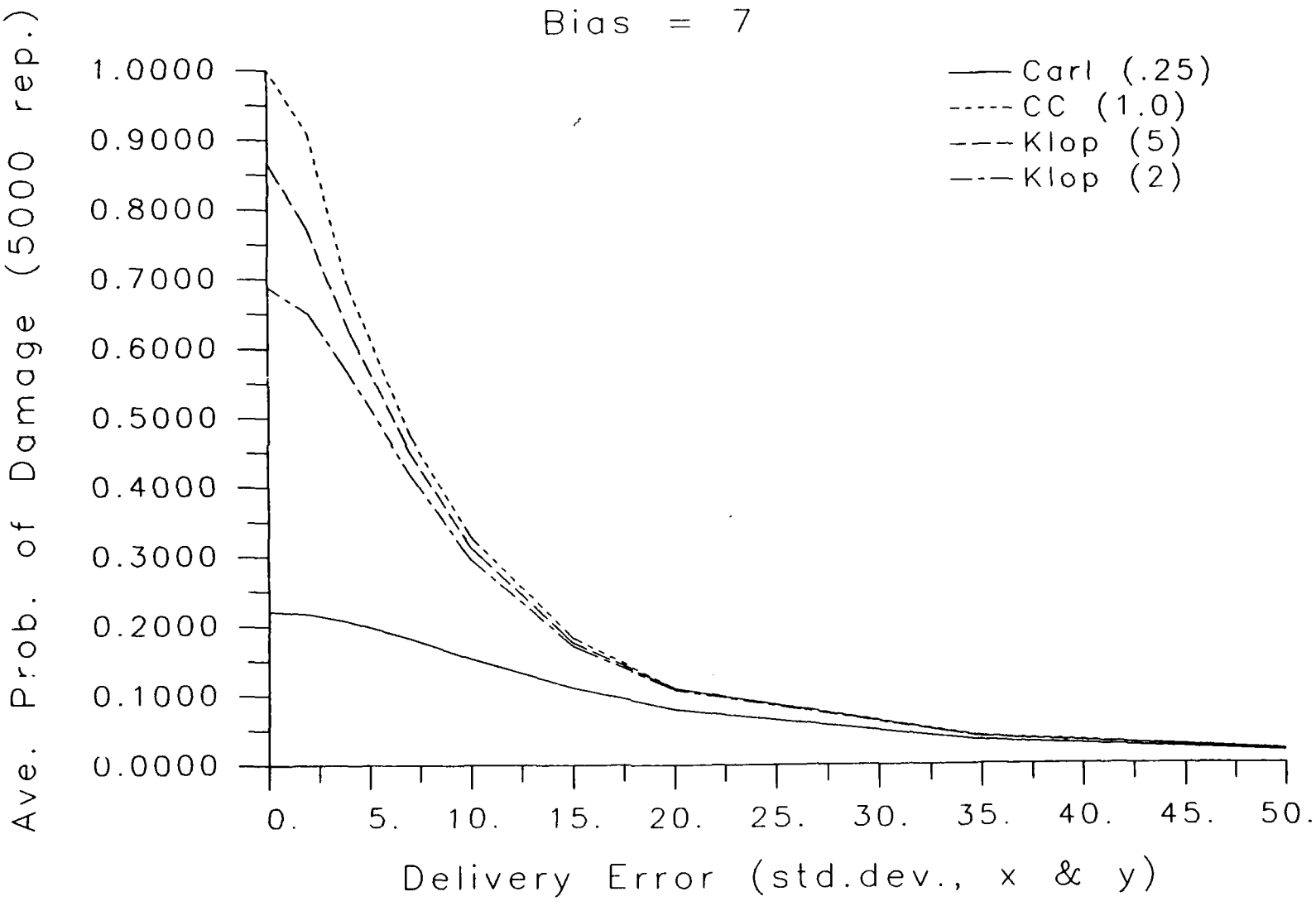

Figure 16: Klopcic, CC and Carleton Results for Aimpoint Bias = 7

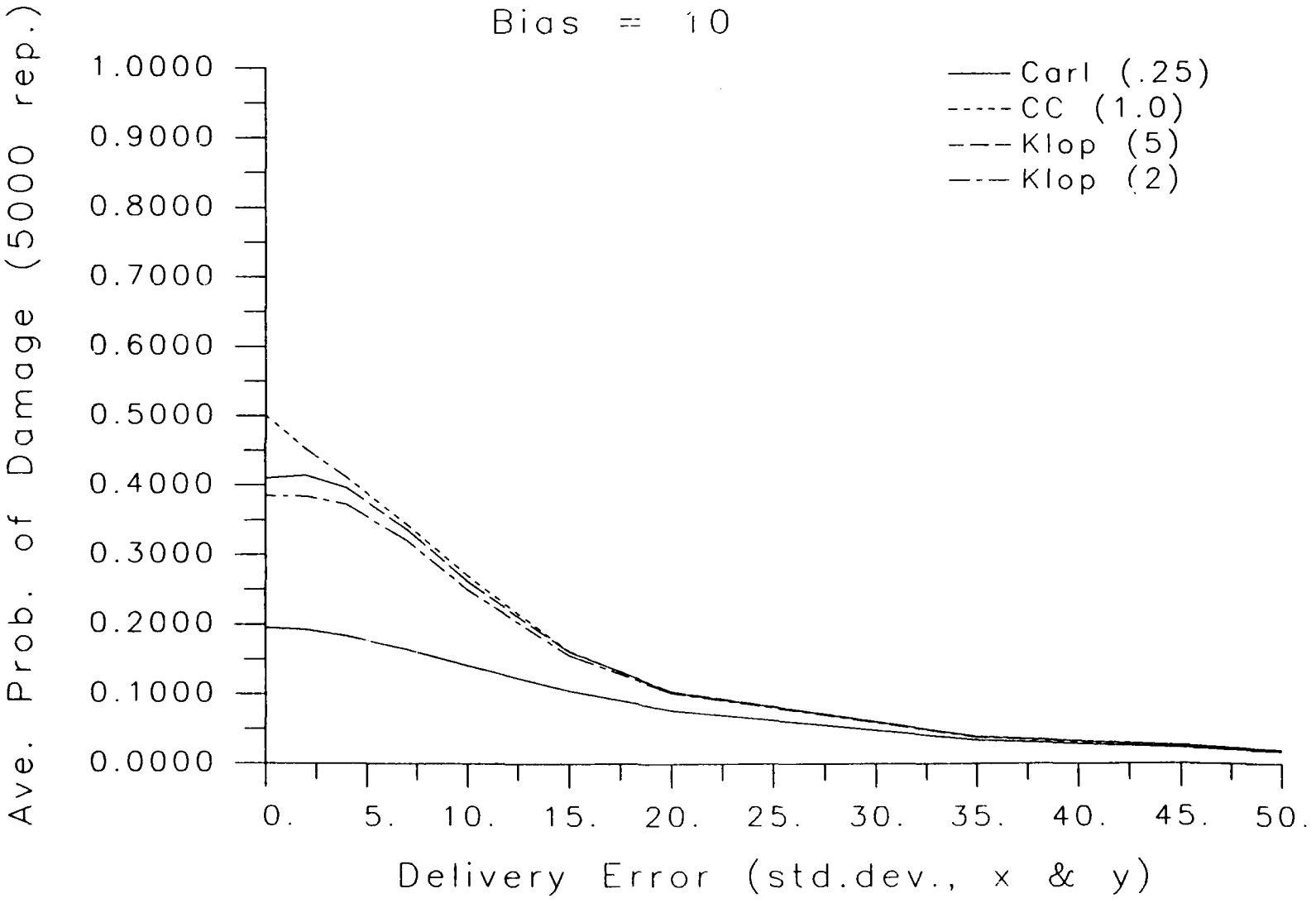

Figure 17: Klopcic, CC and Carleton Results for Aimpoint Bias = 10

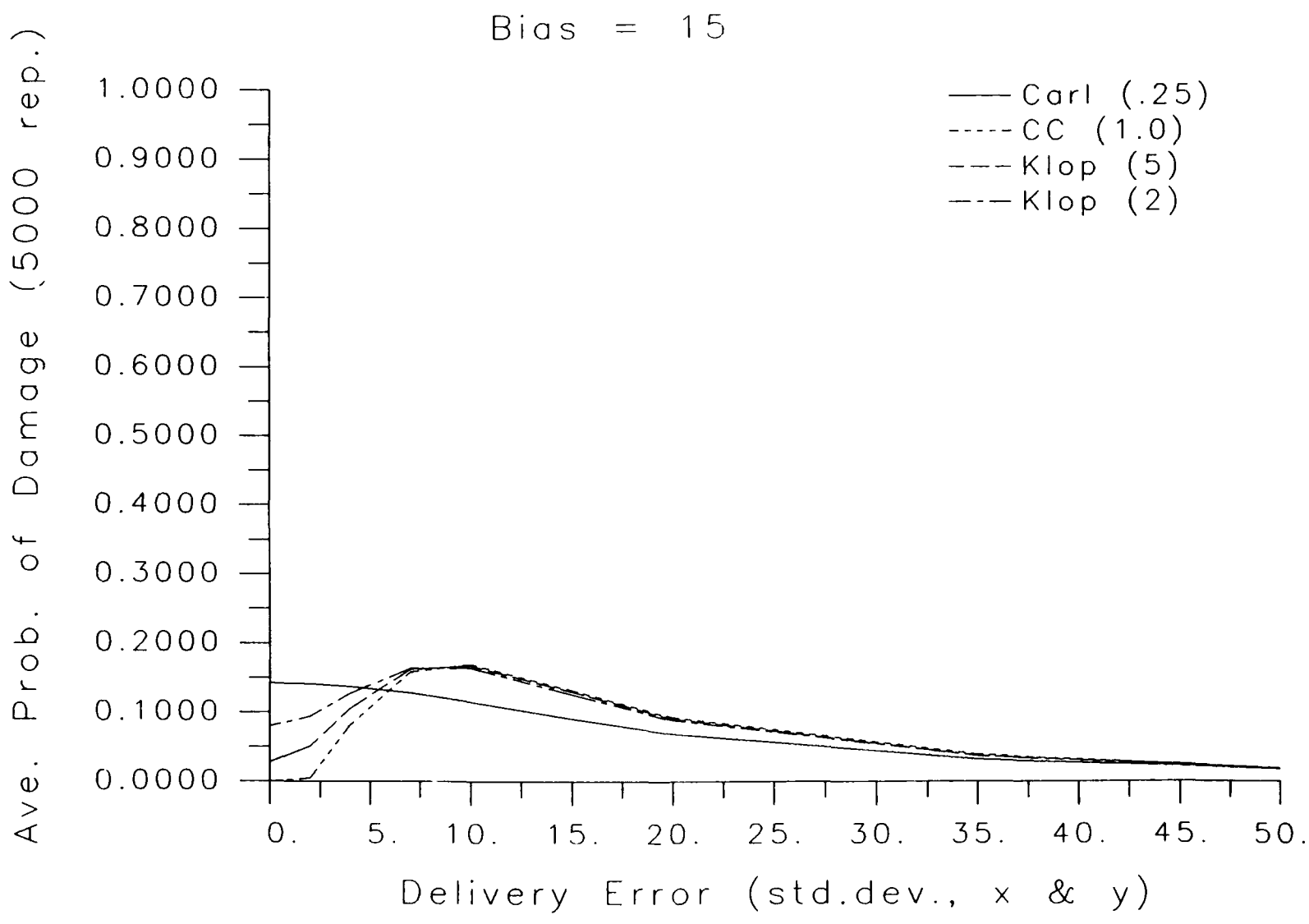

Figure 18: Klopcic, CC and Carleton Results for Aimpoint Bias = 15

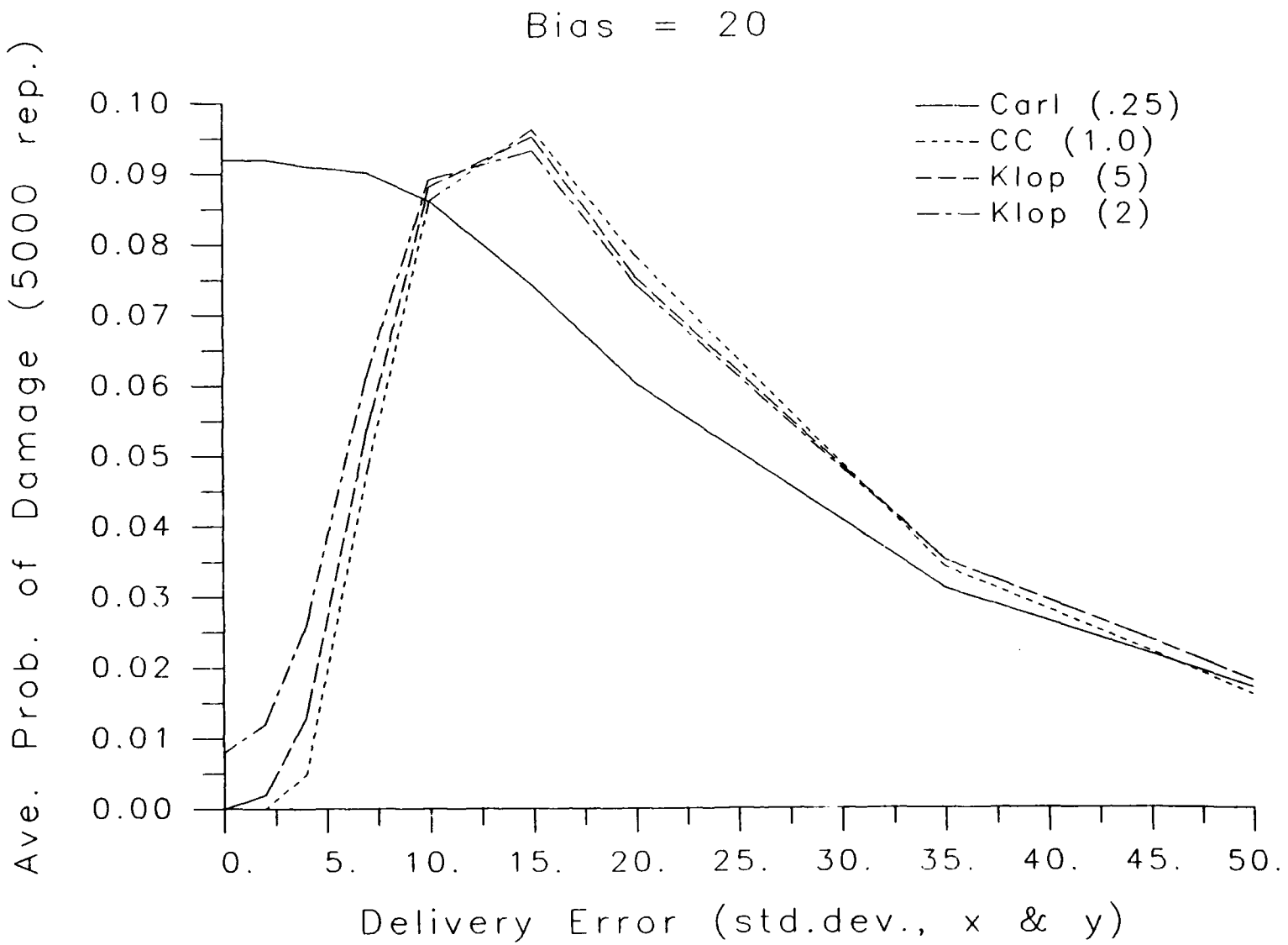

Figure 19: Klopcic, CC and Carleton Results for Aimpoint Bias = 20

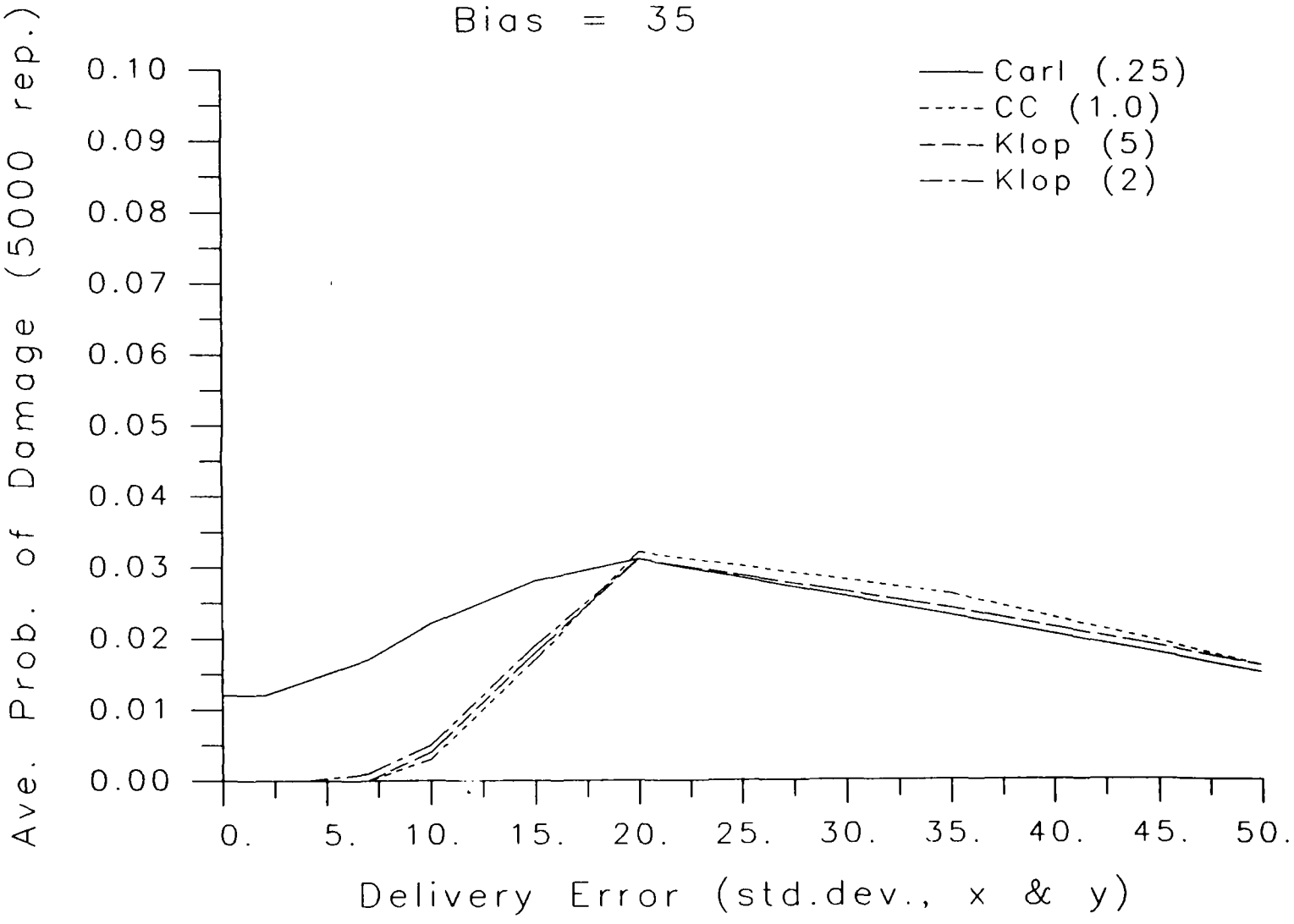

Figure 20: Klopcic, CC and Carleton Results for Aimpoint Bias = 35

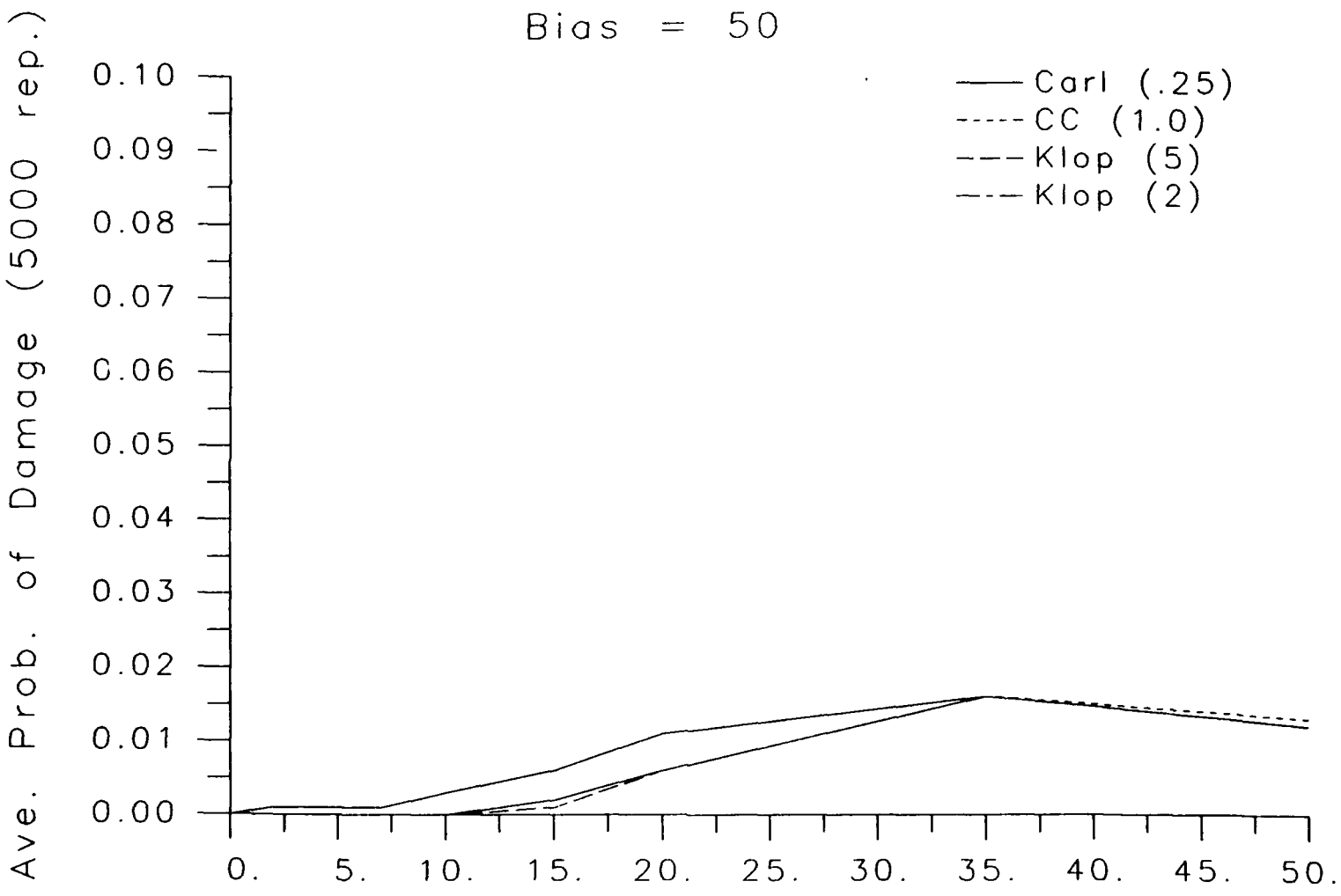

Figure 21: Klopcic, CC and Carleton Results for Aimpoint Bias = 50

C. Summary of Characteristics

The hybrid (Klopcic) function has the desired characteristics set forth in the beginning of this section, viz:

1. It allows a high probability of damage over a specifiable (direct-hit/near-miss) area.
2. It has long, decreasing "tails" to account for the decreasing, but finite, probability of fragment damage with increasing miss distance.
3. It preserves the lethal area of the warhead being modeled.
4. It allows for range-deflection asymmetry in the effects.
5. It is integrable in closed form, allowing easy normalization (to the lethal area).
6. It and its first derivative are continuous.

Unlike the Carleton function, the Klopcic function can not be convoluted in closed form with a (normal) accuracy function. Thus, the Klopcic will be of less use in models such as the "Super-Quickie" models, which rely on a closed form of the equation

$$P_K = \int_{\infty} dA\, P_d(u, v, x, y)\, P_h(x, y) \tag{26}$$

where P_d is the probability of damage of a target at (u,v) due to a weapon at (x,y) and P_h is the probability of a weapon functioning at point (x,y). However, the phenomenal growth and spread of computational power has largely eradicated the need for "Super-Quickie" models with their potential for significant errors that can easily go undetected by the casual user. The run-time and run-cost of inherently more accurate and error-free models (e.g. the Monte Carlo Artillery Effectiveness (MCARTEF) model used in this project) are insignificant considerations.

On the other hand, the Klopcic function provides a simple algorithm for point estimates of damage. The added computation required above that of a Carleton or Cookie Cutter damage function is offset by the ease in input preparation, since the Klopcic function does not require the user to compromise between the lethal and the direct-hit areas. For this reason, it is recommended that this function be incorporated into the more accurate artillery models, as has been done in the MCARTEF model, described in Appendix B.

IV. Summary

In this report, the Carleton and Cookie Cutter (CC) damage functions, commonly used in artillery effectiveness models, have been studied. A number of characteristics of the two functions were demonstrated:

- For an aimpoint on a single target:
  - A simulation using the CC predicts a higher damage probability (Pk) than one using the Carleton.
  - The difference is maximized as the delivery error decreases.
  - The difference disappears as the delivery error increases.
- For aimpoints removed from a single target (bias errors), the relative effectivenesses of the two functions switches (Carleton effectiveness becomes greater than CC). The cross-over point is a complicated function of bias and delivery errors and the lethal area of the weapon being modeled.

Through a series of numerical studies, certain shortcomings of the two damage functions were noted. Most important were:

- The Carleton function significantly underevaluates kills from direct hits and near misses - especially when D_0 (see footnote 2) is set substantially less than 1, which is commonly done for artillery.
- The Cookie Cutter over-estimates the size of the direct-hit/near-miss area and ignores the possibility of kills from distant misses.

To alleviate these shortcomings and produce a damage function that better resembled the analyst's intuitive knowledge of weapon effectiveness, a hybrid function (the Klopcic function) was constructed. It was shown that the Klopcic function retained all the favorable features of the Carleton and CC functions, with the exception of the Carleton's capability for closed-form convolution with a Gaussian function. In addition, the Klopcic function allows direct input of an extra parameter, a direct-hit/near-miss area. This parameter spares the analyst the need to compromise global weapon effectiveness features, such as lethal area, in order to better model an accurate weapon.

To illustrate the behavior of the Klopcic function, the function was compared to the Carleton and CC functions in a series of numerical studies. These studies, like those above, used the new, comprehensive, highly-user-oriented MCARTEF (Monte Carlo ARTillery EFfectiveness) model.

V. Acknowledgements

The author would like to acknowledge the assistance of Mrs. Stephanie Juarascio of the US Army Ballistic Research Laboratory who conducted an extensive series of preparatory computer runs that highlighted the problems addressed in this report.

The author is also particularly grateful for the encouragement, incisive observations and educational conversations with Mr. Richard Sandemeyer of the US Army Materiel Systems Analysis Agency.

Appendix A

Derivation of Lethal Area for the Klopcic Function

This page intentionally left blank

In the main body of this report, the need was shown for a function that more closely resembled the actual damage pattern of a fragmenting munition. In particular, the function must allow for direct hits as well as model the decreasing, but finite probability of fragment damage versus increasing miss distance. A hybrid function, herein referred to as the Klopcic function, was shown to include these features, as well as most of those other features which make the Carleton and Cookie Cutter damage functions so widely useful. To be user-friendly, the input set for the Klopcic function was defined in terms of physically meaningful parameters (rat, Pk_0 and A_{L0}) and the most commonly used measure of effectiveness, A_L. These are defined in Table A-I.

Table A-I: Input parameters for the Klopcic function

A_L:	the total lethal area of the weapon against the target
rat:	A/B, the ratio of x and y extents of the central region
Pk_0:	the probability of damage in the central region
A_{L0}:	the lethal area of the central core

The Klopcic function is defined by:

$$Klopcic\,Function = \begin{cases} Pk_0: & \frac{x^2}{A^2} + \frac{y^2}{B^2} \leq 1. \\ Pk_0\, e^{-[u^2/\sigma_x^2 + v^2/\sigma_y^2]}: & elsewhere \end{cases} \tag{A-1}$$

where:

$$Pk_0, A, B, \sigma_x, \sigma_y = \text{parameters of the distribution} \tag{A-2}$$

$$\frac{A}{B} = \frac{\sigma_x}{\sigma_y} \tag{A-3}$$

$$u = x - x_0 \tag{A-4}$$

$$v = y - y_0 \tag{A-5}$$

$$\frac{x_0^2}{A^2} + \frac{y_0^2}{B^2} = 1. \tag{A-6}$$

$$\frac{x_0}{y_0} = \frac{x}{y} \tag{A-7}$$

The lethal area (for any function) is defined by:

$$A_L = \int_\infty dA\, P_d(u, v, x, y) \tag{A-8}$$

In this appendix, we perform the integration in equation A-8, using the Klopcic function as P_d. The resulting equation yields the relationships needed to relate the input parameters defined above to the functional parameters defined in equations A-1.

We begin by noting that the needed integral breaks into two parts: one inside and one outside the ellipse specified by

$$\frac{x^2}{A^2} + \frac{y^2}{B^2} \leq 1.$$

The inner one is just the lethal area of the direct-hit/near-miss zone. Thus, we need only derive the integral outside of the (AB) ellipse.

A step-by-step solution of the integral is out-of-place in this appendix. Rather, we present some of the intermediate formulae and the conclusion.

First, eliminating x_0 and y_0 from equation A-1 and rearranging makes the "x-part" of the exponent equal to

$$-\frac{x^2}{\sigma_x^2} \times \left(\frac{B^2x^2 + A^2y^2 - 2AB\sqrt{B^2x^2 + A^2y^2} + A^2B^2}{B^2x^2 + A^2y^2} \right) \qquad \text{(A-9)}$$

with a similar expression for the "y-part". Substitution of

$$t = Bx/y$$

significantly reduces the expression. Finally, applying equation A-3 leads to

$$A_L = A_{L0} + Pk_0 \frac{A}{B} \int dt \int dy\, e^{-\frac{(\sqrt{t^2+y^2}-B)^2}{\sigma_y^2}} \qquad \text{(A-10)}$$

where A_{L0} is the lethal area of the direct-hit/near-miss zone. Recall, the double integral is over the area not represented by A_{L0}.

The integral in equation A-10 can be easily transformed, by a change in coordinate systems, to

$$\int_0^{2\pi} d\theta \int_B^{\infty} r\, dr\, e^{-\frac{(r-B)^2}{\sigma_y^2}} \qquad \text{(A-11)}$$

which, in turn, breaks into two standard integrals

$$2\pi \left[\int_0^\infty w\, dw\, e^{-\frac{w^2}{\sigma_y^2}} + B \times \int_0^\infty dw\, e^{-\frac{w^2}{\sigma_y^2}} \right] \qquad \text{(A-12)}$$

Solving, using standard techniques, yields

$$A_L = A_{L0} + \frac{\pi A P k_0}{B} \times \left[\sigma_y^2 + B \sigma_y \sqrt{\pi} \right] \qquad \text{(A-13)}$$

Equation A-13 is the final relationship needed to derive the functional parameters — Pk_0, A, B, σ_x, and σ_y — from the user input parameters: A_L, rat, Pk_0 and A_{L0}. Solving equation A-13 for σ_y and listing the other relationships yields:

$$\sigma_y = \frac{\sqrt{\pi^3 A^2 P k_0^2 - 4\pi \frac{A}{B} P k_0 (A_L - A_{L0})} - \pi^{\frac{3}{2}} A P k_0}{2\pi \frac{A}{B} P k_0} \qquad \text{(A-14)}$$

$$\sigma_x = \text{rat}\, \sigma_y \qquad \text{(A-15)}$$

$$A = \sqrt{\frac{A_{L0}\, \text{rat}}{\pi\, P k_0}} \qquad \text{(A-16)}$$

$$B = \frac{A}{\text{rat}} \qquad \text{(A-17)}$$

With these relationships, the Klopcic function is expressed in terms of the user-friendly, intuitive input parameters listed in Table A-I.

This page intentionally left blank

Appendix B

The MCARTEF Code

This page intentionally left blank

The Monte Carlo ARTillery EFfectiveness (MCARTEF) computer code is a menu-driven program for calculating the probabilities of damage for distributed targets — each with its own damage function — after attack by a set of correlated warheads, such as in an artillery attack. The code, written in standard FORTRAN 77, is immediately transportable to any machine having a FORTRAN compiler in a UNIX environment, and, with little effort, to any FORTRAN-capable computer.

MCARTEF offers a number of options, such as mixing damage function types in the same run. Aimpoints can be input or calculated using standard fire direction algorithms. (Currently, only the Fenderkov algorithm is implemented.) A Monte Carlo technique is used to select actual warhead burst points for each replication. Results can be accumulated deterministically (by averaging the damage probabilities) or stochastically (by drawing a random number against the damage probability).

Four quantities are output. First, the average damage probability is given and the distribution of damage probabilities are plotted for each target. For cases involving more than one target, MCARTEF also plots the distribution of probabilities of damage to at least one target. Finally, for multi-target runs, the probability of damaging various percentages of the target array are plotted.

It is well beyond the scope of this appendix to attempt to produce a user's manual for the MCARTEF code here. However, it was felt useful to present a small demonstration of MCARTEF in order to help the reader determine its utility to his studies.

In this example, the sample runstream which is included in the MCARTEF source deck is loaded. The data are reviewed and an aimpoint is added. The runstream is then executed and the results presented.

It was decided not to print the entire interactive session in the following figures. Rather, a few representative screens and a sample of the results were deemed sufficient for the present purposes.

```
If you want your screen to pause after every few
lines of output, type "Y"

Do you want some on-screen explanations of the code?



MCARTEF INPUT MENU
******************

         TO                                    TYPE
-------------------------------------------------

Read (previously Saved file ..... F
Enter interactive input/edit ..... I
To Review Current Data ..... R

To Save Current Data ..... S

To End Input and Begin Calculation  .. Q

To Quit Run Entirely ..... Z
```

Figure B-1: Opening Screen/Main Menu

```
REVIEW CURRENT DATA MENU
************************

         TO                                  TYPE
-----------------------------------------------

Review Aimpoints ..................... A
Review Damage Functions ............. D
Review Delivery Errors .............. E
Review Firing Unit Data ............. F
Graphical Target Layout ............. G
Review Output Options ............... O
Review Program Controls ............. P
Review Targets ...................... T

To End Review ....................... Q
```

Figure B-2: Review Data Menu

Number of Aimpoints = 4

Aimpoints:

	x	y
1	-5.00	-5.00
2	0.00	5.00
3	5.00	-5.00
4	5.00	0.00

Errors:

	DIST	Range	Deflection
Target Location	normal	40.00	40.00
MPI (Volley Corr.)	unifrm	20.00	50.00
Tube-to-Tube	unifrm	8.00	8.00
Round-to-Round	normal	18.00	12.00

Firing Unit Data:

Number of Firers = 3
Number of Rounds per Firer = 5
Incident angle = 60.00

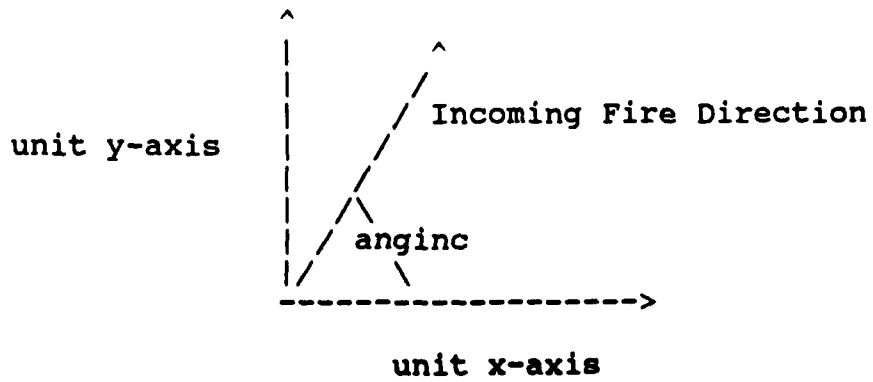

Figure B-3: Data for Sample Run

Number of Damage Functions = 4

Damage Functions:

	type	Name	Parameters AL	rat	D0/Pk0	AL0
1	1	Carlt1	314.16	3.00	0.25	
2	2	Cookie1	314.16	1.00	1.00	
3	1	Carlt2	628.32	2.50	0.30	
4	3	Klop1	314.16	1.00	1.00	101.50

Program Controls:

Number of Replications = 500

Random Number Seeds:
TLE and MPI = 64310
Tube-to-Tube = 4444
Rnd-to-Rnd = 3333
Kills (fully stochastic) = 7398

MODE: Monte Carlo Rounds, Cumulate Damage Probabilities

Number of Targets = 5

Targets:

	Name	DAM. Type	x	y
1	Truck	1	-20.00	-10.00
2	Truck	1	-15.00	-10.00
3	Tank truck	4	0.00	0.00
4	Big truck	3	10.00	8.00
5	Tent	2	0.00	-15.00

Figure B-4: Data for Sample Run, continued

```
Targets Identified by Damage Function Number
y (across) interval =     1.; x interval =     2.
Aimpoints identified by X
INCOMING FIRE DIRECTION FROM :  TO .
*************************************************************************

     -16.          -4.           8.          20.          32.          44.
       V            V            V            V            V            V

  -22.>  :
      >       1
      >          :
      >       1
      >                  :
  -12.>
      >                        :
      >
      >            X                     :
      >
   -2.>                                        .
      > 2               4     X
      >                                             .
      >            X
      >                                                  .
    8.>
      >                        3                                 .
      >
      >
      >

Type any character to continue
```

Figure B-5: Deployment Graphic

```
MCARTEF INPUT/EDIT MENU
***********************



         TO                                  TYPE
-------------------------------------------------

Input/Edit Aimpoints ................. A
Input/Edit Damage Functions ......... D
Input/Edit Delivery Errors .......... E
Input/Edit Firing Unit Data ......... F
Input/Edit Output Options ........... O
Input/Edit Program Controls ......... P
Input/Edit TARGETS .................. T

To Review Current Data ............. R

To End Input/Edit ................... Q
```

Figure B-6: Edit Menu

```
FIRING UNIT MENU
****************

     TO                                              TYPE
 ------------------------------------------------------
 Input the incident angle ..................... A
 Input the number of guns/Aimpoints ........ G
 Input the number of rounds per gun ........ N
 Review current data ....................... R

 Quit and return to input menu ............. Q


 The Number of Guns is input by inputting an aimpoint
 For each gun



AIMPOINT MENU
*************

     TO                                    TYPE
 ------------------------------------------------
 Add more aimpoints ................ A
 Delete aimpoints .................. D
 Generate aimpoints (FENDERKOV) .... F
 Review current aimpoints .......... R

 Quit and return to input menu ..... Q
```

Figure B-7: Typical Lower Level Menus (Firing Unit and Aimpoint)

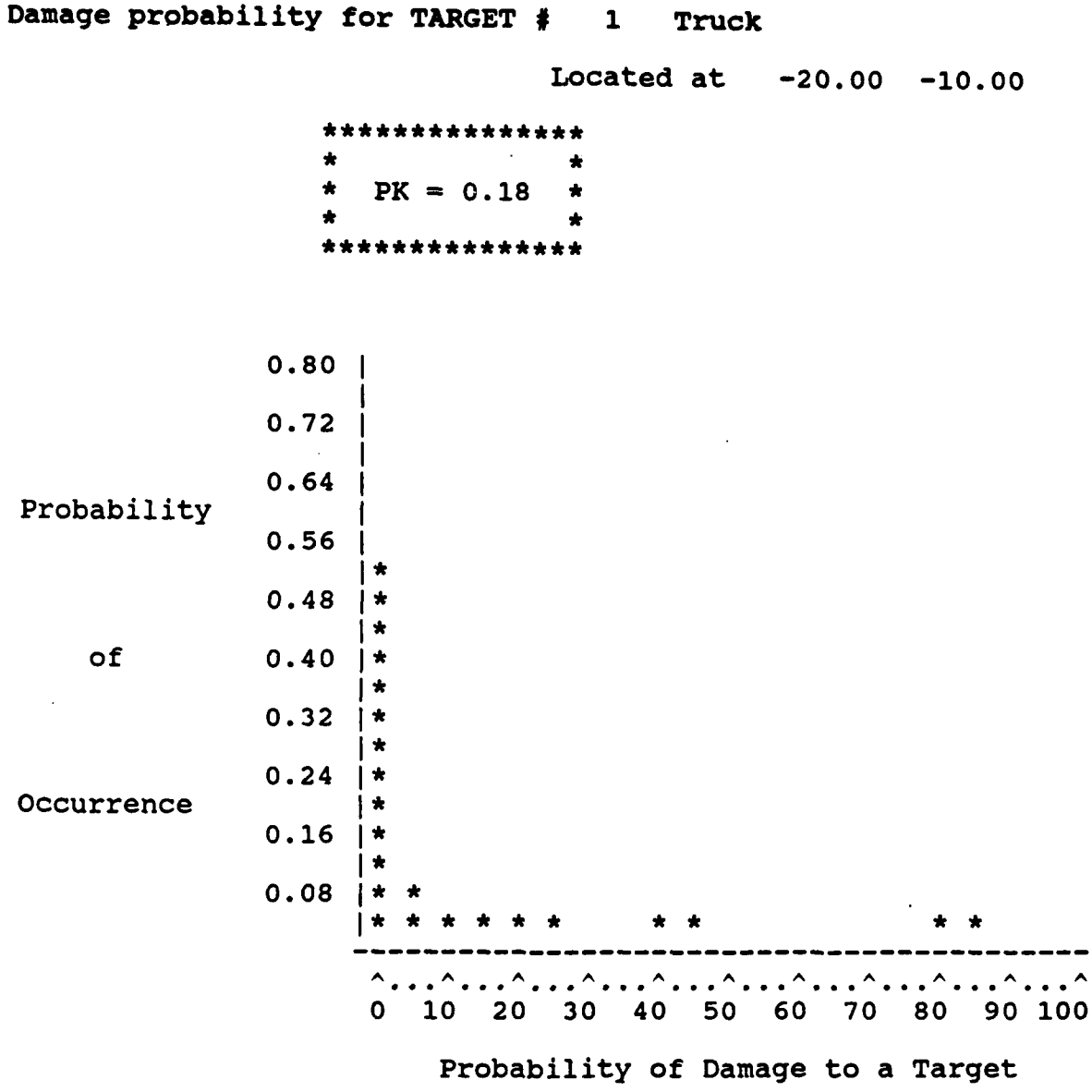

Figure B-8: Damage Probability for Target #1

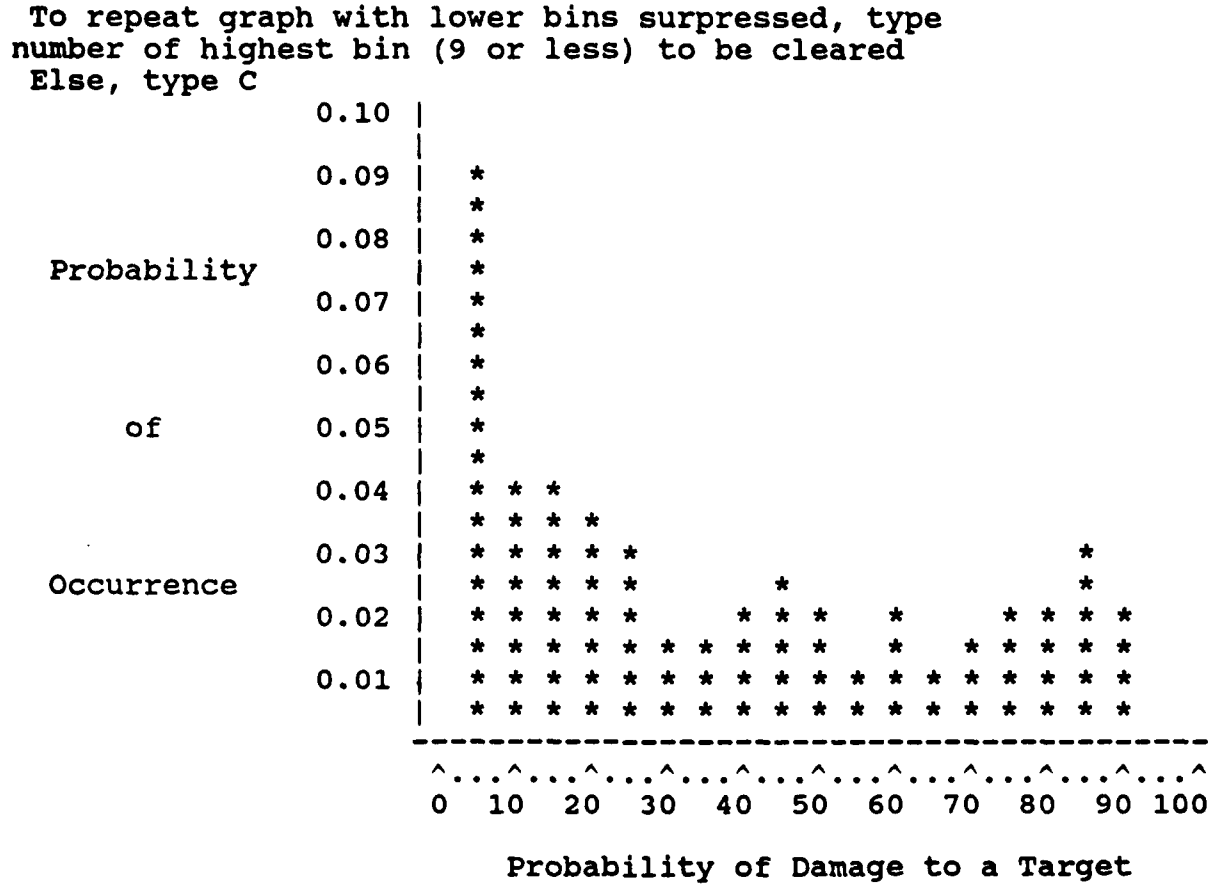

Figure B-9: Damage Probability, Rescaled, with Column 1 Removed

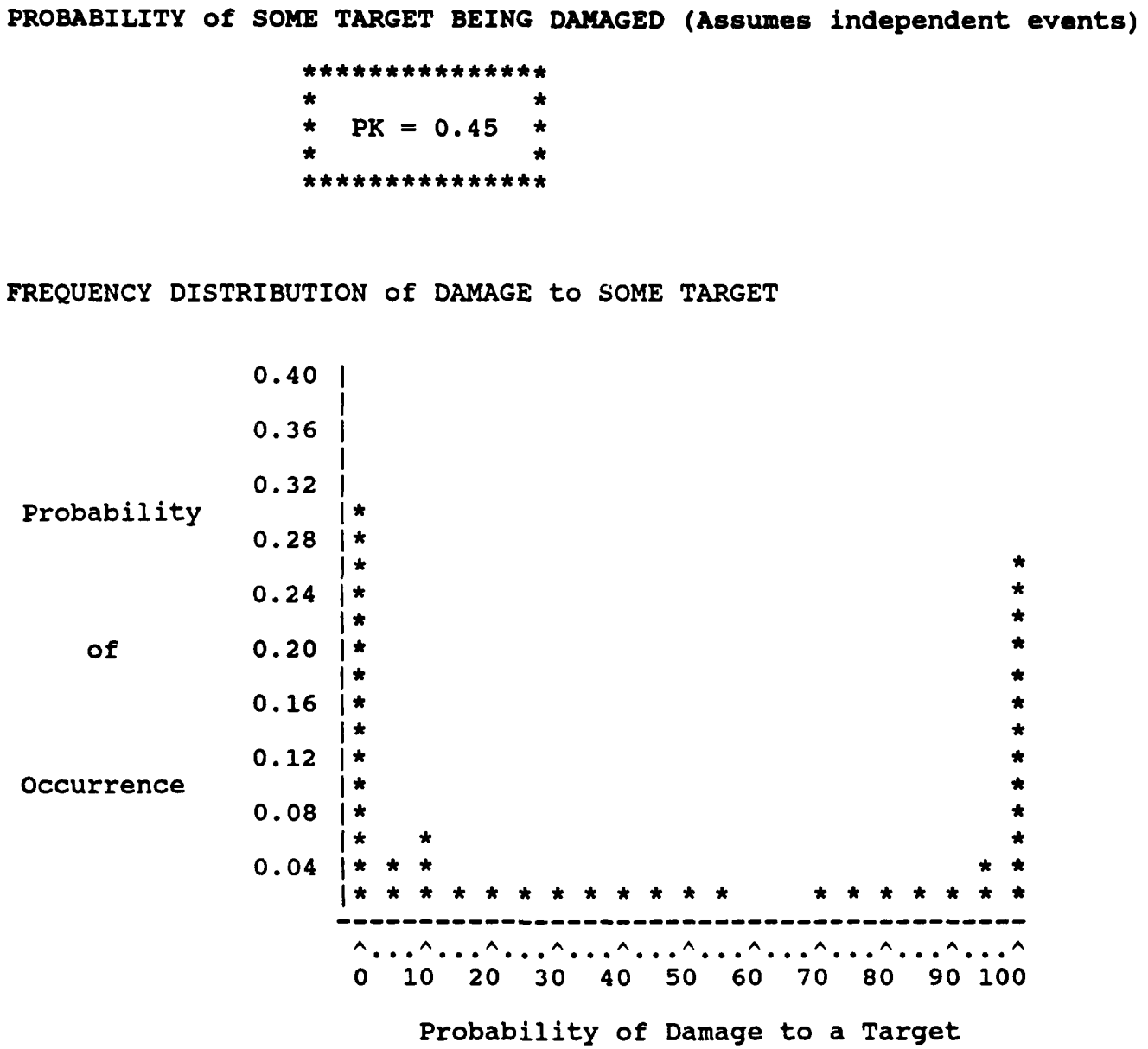

Figure B-10: Probability of Some Damage

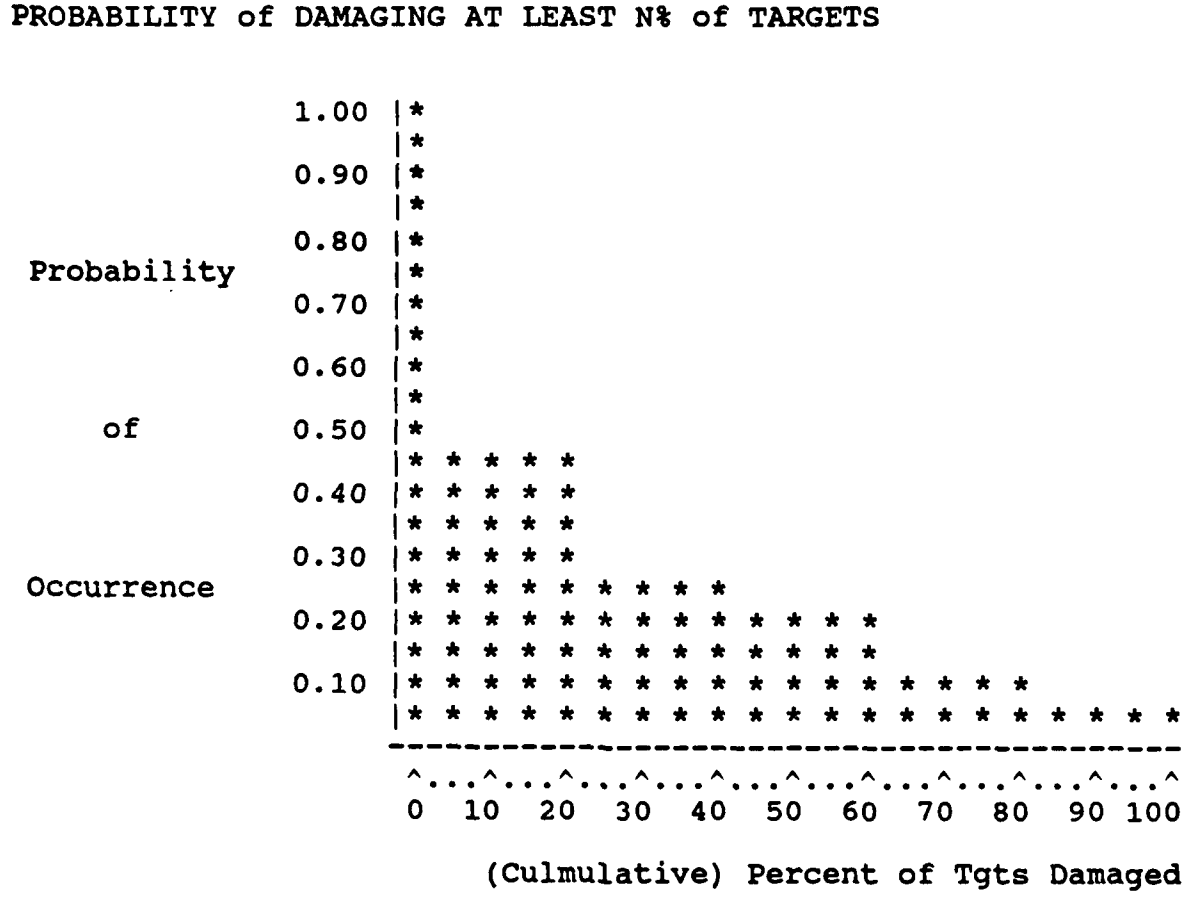

Figure B-11: Cumulative Damage Probability Plot

TABLE of CUMULATIVE DAMAGE

% DMG	PROB	% DMG	PROB
5	0.448	55	0.184
10	0.448	60	0.184
15	0.448	65	0.088
20	0.448	70	0.088
25	0.274	75	0.088
30	0.274	80	0.088
35	0.274	85	0.040
40	0.274	90	0.040
45	0.184	95	0.040
50	0.184	100	0.040

Figure B-12: Cumulative Damage Probability Table

INTENTIONALLY LEFT BLANK.

No of Copies	Organization
1	Office of the Secretary of Defense OUSD(A) Director, Live Fire Testing ATTN: James F. O'Bryon Washington, DC 20301-3110
2	Administrator Defense Technical Info Center ATTN: DTIC-DDA Cameron Station Alexandria, VA 22304-6145
1	HQDA (SARD-TR) WASH DC 20310-0001
1	Commander US Army Materiel Command ATTN: AMCDRA-ST 5001 Eisenhower Avenue Alexandria, VA 22333-0001
1	Commander US Army Laboratory Command ATTN: AMSLC-DL Adelphi, MD 20783-1145
2	Commander US Army, ARDEC ATTN: SMCAR-IMI-I Picatinny Arsenal, NJ 07806-5000
2	Commander US Army, ARDEC ATTN: SMCAR-TDC Picatinny Arsenal, NJ 07806-5000
1	Director Benet Weapons Laboratory US Army, ARDEC ATTN: SMCAR-CCB-TL Watervliet, NY 12189-4050
1	Commander US Army Armament, Munitions and Chemical Command ATTN: SMCAR-ESP-L Rock Island, IL 61299-5000
1	Commander US Army Aviation Systems Command ATTN: AMSAV-DACL 4300 Goodfellow Blvd. St. Louis, MO 63120-1798

No of Copies	Organization
1	Director US Army Aviation Research and Technology Activity Ames Research Center Moffett Field, CA 94035-1099
1	Commander US Army Missile Command ATTN: AMSMI-RD-CS-R (DOC) Redstone Arsenal, AL 35898-5010
1	Commander US Army Tank-Automotive Command ATTN: AMSTA-TSL (Technical Library) Warren, MI 48397-5000
1	Director US Army TRADOC Analysis Command ATTN: ATAA-SL White Sands Missile Range, NM 88002-5502
(Class. only) 1	Commandant US Army Infantry School ATTN: ATSH-CD (Security Mgr.) Fort Benning, GA 31905-5660
(Unclass. only) 1	Commandant US Army Infantry School ATTN: ATSH-CD-CSO-OR Fort Benning, GA 31905-5660
1	Air Force Armament Laboratory ATTN: AFATL/DLODL Eglin AFB, FL 32542-5000
	Aberdeen Proving Ground
2	Dir, USAMSAA ATTN: AMXSY-D AMXSY-MP, H. Cohen
1	Cdr, USATECOM ATTN: AMSTE-TD
3	Cdr, CRDEC, AMCCOM ATTN: SMCCR-RSP-A SMCCR-MU SMCCR-MSI
1	Dir, VLAMO ATTN: AMSLC-VL-D

No of Copies	Organization
1	HQDA ATTN: DAMO-ZD (Mr. Riente) The Pentagon, Room 3E360 Washington, DC 20310
2	OSD OUSD (A) ODDDRE (T&E/LFT) ATTN: James O'Bryon Albert E. Rainis The Pentagon, Room 3E1060 Washington, DC 20301-3110
2	Deputy Under Secretary of the Army for Operations Research ATTN: DUSA-OR (Walt Hollis) The Pentagon, Room 2E660 Washington, DC 20310-0102
2	Commander US Army Laboratory Command ATTN: AMSLC-CT (J. Predham, D. Smith) 2800 Powder Mill Road Adelphi, MD 20783-1145
1	Commander US Army Laboratory Command ATTN: AMSLC-TD (R. Vitali) 2800 Powder Mill Road Adelphi, MD 20783-1145
1	Commander Armament RD&E Center ATTN: SMCAR-FSS-E (Jack Brooks) Picatinny Arsenal, NJ 07806-5000
1	Administrative Support Group Office Secretary of the Army Room 3D715, Pentagon Bldg. Washington, DC 20310
1	Headquarters, Department of the Army OASA (RDA) ATTN: SARD-IP (Mr. Woodall) Washington, DC 20310-0103
1	Headquarters, Department of the Army Military Deputy to the Assistant Secretary of the Army for RD&A ATTN: SARD (LTG Pihl) Washington, DC 20310
3	Headquarters, Department of the Army ODCSOPS ATTN: DAMO-FDZ (MG Granrud) DAMO-FDT (Mr. Shrader) DAMO-FDG (COL Reed) Washington, DC 20310-0460
2	Headquarters, Department of the Army ODCSINT ATTN: DAMI-ZC (BG Stewart) DAMI-FIT-ST (MAJ Greene) Pentagon, Room 2E453 Washington, DC 20310-1087
1	Headquarters, Department of the Army ODCSLOG ATTN: DALO-2 (MG Rosier) Washington, DC 20310
1	Headquarters, Department of the Army DCSLOG ATTN: DALO-SMP-M (LTC Casey) Washington, DC 20310
2	Headquarters, US Army Training and Doctrine Command ATTN: ATCD-ZA (BG (P) Silvasy) Dir Firepower (COL Rogers) Fort Monroe, VA 23651
1	Commandant US Army Field Artillery School ATTN: ATSF-CCT (COL Anderson) Fort Sill, OK 73503-5600
1	Commandant US Army Field Artillery School ATTN: ATSF-TSM-CN (COL Reece) Fort Sill, OK 73503-5006
2	Commandant US Army Armor School ATTN: ATZK-CG (MG Foley) ATSB-CD-TE (LTC Tremmel) Fort Knox, KY 40121-5000
1	Commandant US Army Armor School ATTN: ATSB-TSMT (COL Colgan) Fort Knox, KY 40121-5201
1	Commandant US Army Infantry School ATTN: ATSH-CMT (MG Spigelmire) Fort Benning, GA 31905-5000
1	Commandant US Army Infantry School ATTN: TSM-Bradley Fighting Vehicle Systems (COL Hixon) Fort Benning, GA 31905-5592
2	Commander US Army Materiel Command ATTN: AMCDE (Dr. Oscar) AMCSM-MME (Mr. Davis) 5001 Eisenhower Avenue Alexandria, VA 22333-0001

No of Copies	Organization
4	Commander US Army Operational Test and Evaluation Agency ATTN: CSTE-ZT (MG Stephenson, Mr. Dubin) CSTE-CCR (LTC Crupper) CSTE-FS (COL Wall) 4501 Ford Avenue Alexandria, VA 22302-1458
6	Commander US Army Tank-Automotive Command ATTN: PEO-HFM (BG (P) McVey) APEO-HFM (BG Hite) AMCPM-ABMS (COL Longhouser) AMCPM-BFVS (Mr. Chamberlain) AMCPM-SS (Mr. Dean) AMSTA-M (COL Manners) Warren, MI 48397-5000
1	Commander US Army Combined Arms Center ATTN: ATZL-TIE (Mr. Bruchette) Fort Leavenworth, KS 66027-5310
1	Commander US Army FSTC ATTN: AIFRCA (Mr. Holthus) 220 Seventh St. NE Charlottesville, VA 22901-5396
1	Commander Test and Experimentation Command ATTN: ATCT-MA (MAJ Anderson) Fort Hood, TX 76543
1	Commander US Army TRADOC Analysis Center ATTN: ATRC-WD (Mr. Shugart) White Sands Missile Range, NM 88002-5002
1	Commander US Army NATICK Research Development and Engineering Center ATTN: STRNC-ICAA (Ms. Mooney) Natick, MA 01760-5019
1	Commander US Army Missile Command ATTN: AMCPEO-FS (BG Schumacher) Redstone Arsenal, AL 35898-5000
1	Commander TRADOC Analysis Center ATTN: ATRC (COL (P) Howard) Ft. Leavenworth, KS 66027-5200

No of Copies	Organization
1	Commander US Army Combined Army Training Agency ATTN: ATZL-TA (BG Mullen) Ft. Leavenworth, KS 66027-7000
1	Commander US Army Combined Arms Combat Developments Activity ATTN: ATZL-CAB (TPIO-HFM, MAJ Jones) Ft. Leavenworth, KS 66027
1	Commander US Army Logistics Center ATTN: ATCL-MRI (MAJ Brown) Ft. Lee, VA 23801-6000
2	Director Walter Reed Army Institute for Research ATTN: SGRD-UWH-E (MAJ Ripple) Washington, DC 20307-5100
1	Director Vulnerability/Lethality Assessment Management Office ATTN: Mr. Gary Holloway Building 459, Room 329 Aberdeen Proving Ground, MD 21005-5001
1	Director US Army Concepts Analysis Agency ATTN: CSCA-ZA (Mr. Van Diver) Bethesda, MD 20814

Aberdeen Proving Ground

Dir, USAMSAA
ATTN: AMXSY-G, J. Kramer, Mr. Dibelka
AMXSY-GA, W. Brooks
AMXSY-J, A. LaGrange
AMXSY-GS, Mr. King
AMXSY-LA, LTC Jensen
AMXSY-GI, CPT Klimack
AMXSY-IM, Mr. Steiner
AMXSY-A, Mr. Puckey
AMXSY-C, Mr. Sandemeyer
AMXSY-D, Mr. Myers

Cdr, USATECOM
ATTN: AMSTE-LFT
AMSTE-TE (R. Pollard)
AMSTE-TA-L (Mr. Yankalonis)

Cdr, USAOCS
ATTN: ATSL-CMT (BG (P) Ball)
ATSL-CD (COL Roberts)
ATSL-TD (COL Salter)

INTENTIONALLY LEFT BLANK.

USER EVALUATION SHEET/CHANGE OF ADDRESS

This Laboratory undertakes a continuing effort to improve the quality of the reports it publishes. Your comments/answers to the items/questions below will aid us in our efforts.

1. BRL Report Number BRL-MR-3823 Date of Report APRIL 1990

2. Date Report Received _____

3. Does this report satisfy a need? (Comment on purpose, related project, or other area of interest for which the report will be used.) _____

4. Specifically, how is the report being used? (Information source, design data, procedure, source of ideas, etc.) _____

5. Has the information in this report led to any quantitative savings as far as man-hours or dollars saved, operating costs avoided, or efficiencies achieved, etc? If so, please elaborate. _____

6. General Comments. What do you think should be changed to improve future reports? (Indicate changes to organization, technical content, format, etc.) _____

CURRENT ADDRESS

Name

Organization

Address

City, State, Zip Code

7. If indicating a Change of Address or Address Correction, please provide the New or Correct Address in Block 6 above and the Old or Incorrect address below.

OLD ADDRESS

Name

Organization

Address

City, State, Zip Code

(Remove this sheet, fold as indicated, staple or tape closed, and mail.)

FOLD HERE

DEPARTMENT OF THE ARMY
Director
U.S. Army Ballistic Research Laboratory
ATTN: SLCBR-DD-T
Aberdeen Proving Ground, MD 21005-5066
OFFICIAL BUSINESS

NO POSTAGE
NECESSARY
IF MAILED
IN THE
UNITED STATES

BUSINESS REPLY MAIL
FIRST CLASS PERMIT No 0001, APG, MD

POSTAGE WILL BE PAID BY ADDRESSEE

Director
U.S. Army Ballistic Research Laboratory
ATTN: SLCBR-DD-T
Aberdeen Proving Ground, MD 21005-9989

FOLD HERE